Physics of pulsar magnetospheres

V. S. Beskin, A. V. Gurevich, and Ya. N. Istomin

P. N. Lebedev Physics Institute, Academy of Sciences of the USSR, Moscow

Usp. Fiz. Nauk **150**, 257–298 (October 1986)

A self-consistent model of the magnetosphere of a pulsar is constructed. This model is based on a successive solution of the equations describing global properties of the magnetosphere and on a comparison of the basic predictions of the developed theory and observational data.

CONTENTS

1. PULSARS; BASIC OBSERVATIONAL CHARACTERISTICS

Pulsars or, more precisely, radiopulsars—sources of pulsed radio waves received from space—were discovered in 1967 by some English radio astronomers[1] and were identified essentially immediately with rotating neutron stars.[2] Such stars should form as a result of the collapse (a catastrophic gravitational contraction) of ordinary stars which have exhausted their reserve of nuclear fuel. In neutron stars, the gravitational forces are balanced not by the gas pressure, as in ordinary stars, but by the pressure of degenerate electrons, as in white dwarfs, and by the pressure of the highly compressed neutron matter. These entities are therefore huge blobs of nuclear matter, and at a mass of the order of the solar mass they should have a radius $R \sim 10$ km (Ref. 3).

The experimental observation of pulsars, i.e., of neutron stars, which had been predicted back in the mid-1930s,[4] is rightly regarded as one of the major discoveries in astrophysics. For this discovery, Antony Hewish was awarded the Nobel prize in 1974.

The discovery of radiopulsars was followed immediately by the observation of several other cosmic entities (x-ray pulsars,[5] sources of x-ray[6] and γ-ray bursts,[7] and other entities[8–10]), whose activity is also linked with processes which occur in neutron stars.[11–13] A discussion of the nature of those sources, however, goes beyond the scope of the present review.

Radiopulsars are presently being studied at essentially all the leading observatories around the world. In particular, the list of observed sources is continually growing. By mid-1986, 437 pulsars had been found. The total number of radiopulsars in the Local Galaxy, on the other hand, is of the order of[14] 100 000. The number of pulsars which have become "extinguished," i.e., the number of neutron stars which are no longer emitting in the radio range, should be three orders of magnitude greater.

The average distances to the pulsars known to us are 0.3–3 kpc. These distances are a hundred times greater than the distances to the nearest stars. Like ordinary stars, pulsars are concentrated near the galactic plane, but the thickness of the stellar disk is slightly smaller than that of the pulsar disk[15] (~ 500 pc). We might also note that the intrinsic velocities of pulsars reach[16] 200–400 km/s, significantly higher than the average velocities of ordinary stars.

Finally, pulsars are, in addition to everything else, exceptionally effective probes of the interstellar medium. They send us their pulses of radio waves over a broad frequency range and at strictly determined times. By studying the retardation, the absorption, and the change in the polarization

 0038-5670/86/100946-25S01.80

of these pulses we can determine the properties of the interstellar medium. It is this approach which has given us the most accurate information on the interstellar gas, on the magnetic field of the Local Galaxy, and on the distance scale. This approach has also made it possible to carry out other extremely accurate measurements.[17–20]

Among the basic observational characteristics of radiopulsars we should classify the period (P) of the pulsar, the spectrum and polarization of the radio emission, and the shape of the mean profile. These characteristics serve as "technical specifications" of each pulsar.

1.1. Periods of pulsars. The radio emission from pulsars arrives here in distinct bursts or pulses. The time interval between pulses is called the "period" P of the pulsar. The periods of all known pulsars lie between 0.00 156 s and 4.3 s; the overwhelming majority fall in the narrower interval 0.3–1.5 s (Ref. 21). The value of P for each pulsar is a constant to six or more significant figures. For example, the period of the fastest millisecond pulsar, PSR 1937 + 21,

$$P = 0.0\ 015\ 578\ 064\ 488\ 724 \text{ s}$$

is presently known to 13 significant figures, and the stability of this frequency is at the level of the best atomic standards.[22] There is talk of introducing a new, "pulsar," time scale to make use of this surprising property.[23]

The existence of this strict periodicity in the repetition of pulses was a governing factor in the construction of the pulsar model shown in Fig. 1 (Ref. 2). This model has the pulsar period P being equal to simply the rotation period of the neutron star. Indeed, only the rotation of an exceedingly compact star could explain both the very short periods of pulsars and the high stability of the repetition of pulses.

An important point is that the periods of all pulsars are gradually increasing. The rate of change of the period, dP/dt, has now been determined for 300 pulsars. The values of the derivative dP/dt are stable, and for most pulsars they lie between[24] 10^{-14} and 10^{-16}. The time scale of the slowing of the rotation,

$$\tau_P = \frac{P}{2\dot{P}}, \qquad (1.1)$$

is actually the lifetime of the radio pulsar. It is typically a few million years.[25]

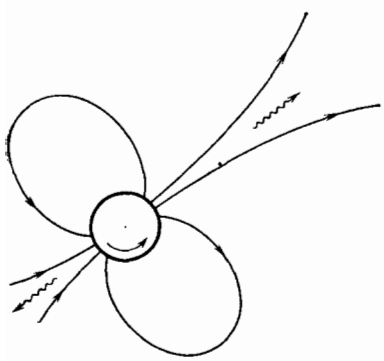

FIG. 1. Model of a pulsar: a rotating neutron star. The arrows show the region in which the directed radio emission is generated.

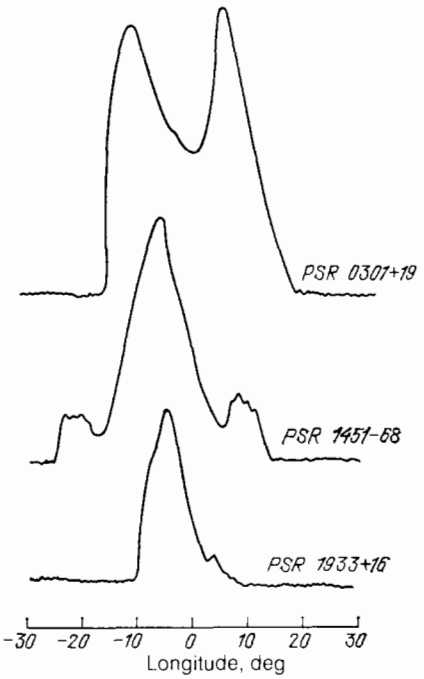

FIG. 2. Typical mean profiles of the radio emission of pulsars.[26]

1.2. Mean profile. Another characteristic feature of the emission of a pulsar is its high directionality. If we assume that the pulsar period P corresponds to a 360° rotation, we would conclude that the typical width of the directional pattern of a pulsar, W_r, is only 10°–30°. For only a few pulsars does the radio emission occupy a significant fraction of the total period P. Figure 2 shows some examples of the shape of the mean profiles of the emission of pulsars.[26]

The mean profiles in Fig. 2 correspond to an average over several hundred successive pulses. Such mean profiles have a shape characteristic of each pulse, are stable, and are independent of the time. The shape of the individual pulses, in contrast, may differ greatly from the shape of the mean profile. The structure of the individual pulses is rather complex. In particular, subpulse details (with a time scale ~ 10 ms) and microstructural details (with a time scale ~ 100 μs) have now been reliably identified.[27,28] These details do not survive on the mean profile.

1.3. Polarization. The radio emission of pulsars is characterized by high polarization. The linear polarization reaches 100% in some subpulses, while the average degree of linear polarization is 30–50% (Ref. 29). In some cases, but far more rarely, circular polarization is observed.[30]

Figure 3 shows a typical time evolution of the position angle of the linear polarization (i.e., of the angle between the direction of the electric field of the wave and a given direction lying in the visual plane).[25] For some pulsars, the total rotation of the position angle reaches 180°. Furthermore, it is frequently possible to distinguish two orthogonal modes in the radio emission,[31] differing in both position angle and the direction of the circular polarization.

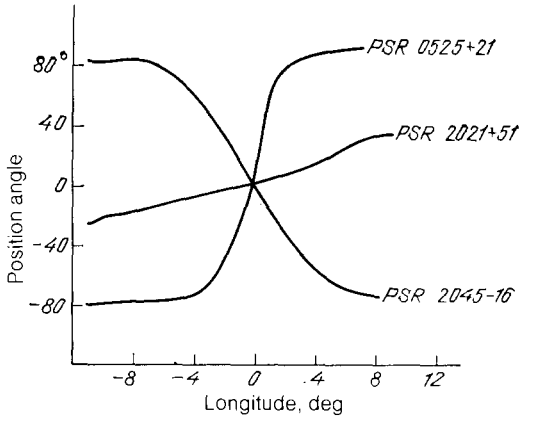

FIG. 3. Changes in the position angle of the linear polarization within the mean profile.[25]

1.4. Energetics of pulsars. The radio emission of pulsars is received over a broad frequency range, from 30 MHz to 10 GHz, i.e., at essentially all the radio wavelengths which can pass through the earth's ionosphere and atmosphere. The frequency spectra of the radio emission are described over a broad range by a power law $I_\nu \propto \nu^{-\bar{\alpha}}$ with an index $\bar{\alpha} \approx 0.6$–2.[32,33] There is a high-frequency drop-off (at $\nu > 10$ GHz), and there is also a low-frequency drop-off ($\nu < 10$ MHz).[33]

An exceedingly important property of the observed radio emission is its high brightness temperature. In radio astronomy it is common to use not the value of I_ν but the brightness temperature T_b, defined as the temperature of a black body which would provide the same emission intensity I_ν. It turns out that the brightness temperature of pulsars, T_b, is of the order of 10^{21}–10^{25} K and even reaches 10^{30} K in some cases.[25] The radio emission of pulsars thus cannot be a thermal emission. Furthermore, the high brightness temperature is unambiguous evidence that the mechanism for the generation of the radio emission must be coherent (Ginzburg *et al.*[34,35]).

The integrated emission power of pulsars in the radio range is extremely high: of the order of 10^{26}–10^{30} erg/s. However, the emission of pulsars is not confined to the radio range: For four pulsars, intense emission has been observed in other parts of the electromagnetic spectrum.[25] For example, emission from the pulsar PSR 0531 + 21, in the Crab Nebula (period $P = 0.033$ s), is also detected in the IR, optical, x-ray, and γ-ray ranges, with γ-ray energies up to 10^{13} eV (Refs. 36 and 37). The total power radiated by this pulsar reaches 10^{37} erg/s—four orders of magnitude greater than that of the radiation from the sun. Nuclear burning does not occur in a neutron star. What is the source of the energy required to sustain this high activity of pulsars?

The answer to this question is known. As we have already mentioned, the periods of all pulsars are increasing; i.e., the rotational velocity of the neutron star is decreasing. Calculating the energy released in the process from

$$W = -I_r \Omega \dot{\Omega}, \tag{1.2}$$

where $I_r \sim 10^{45}$ g·cm^2 is the moment of inertia of the neutron star, and $\Omega = 2\pi/P$ is the angular velocity of the rotation, we find the loss to be 10^{30}–10^{40} erg/s. This loss is always greater than the energy involved in the observed emission.

These are the basic observational characteristics of radiopulsars. We see that even a preliminary analysis of these characteristics reveals both the nature of the pulsars and the energy source of their activity. It is also natural to suggest that the high coherence and directionality of the emission are due to a strong magnetic field (Fig. 1) and to the plasma near the neutron star, i.e., the magnetosphere of the pulsar, in which this radiation is generated.[38]

Many questions of course arise here. Why does a rotating neutron star slow down, and what is the mechanism for this slowing? What is this magnetospheric plasma? Where does it come from? How is part of the energy of the slowing of the star transformed into radiation energy? What is the mechanism for the generation of the coherent and highly directional radio emission? Despite the serious efforts of theoreticians, these questions have yet to be comprehensively answered.[21,25,39]

The situation has recently been changing substantially. It has become possible to construct a systematic theory for the physics of the magnetosphere of a neutron star. This theory explains, in a unified way, the slowing of the pulsars,[40,41] the release of the energy of the slowing in active regions,[41,42] the production of plasma,[42–44] and the generation of the directional radio emission.[45] Our purpose in this review is to set forth the present state of this theory.

2. PHYSICAL PROCESSES IN THE MAGNETOSPHERE OF A PULSAR

In this section we will take a qualitative look at the nature of the basic physical processes which occur in the magnetosphere of a pulsar. We recall that both the theories for the formation and evolution of neutron stars[46,47] and certain direct observations[48] show that the magnetic field B_0 near the surface of the star reaches a level of 10^{11}–10^{13} G. Because of the rotation, an electric field also arises. It can be estimated to be

$$E_{c0} \approx \frac{\Omega R}{c} B_0 \sim 10^{10} - 10^{12} \text{ V/cm}; \tag{2.1}$$

here Ω is the angular velocity of the rotation of the star, R is its radius, and c is the velocity of light. An important point is that since the surface of the star is polarized the electric field also has a component parallel to the magnetic field.[38] Particles entering such a strong electric field are accelerated, and they emit hard γ rays. As these γ rays are absorbed in the magnetic field, they produce electron-positron pairs.[43] In this way, the magnetosphere of the pulsar forms. The electron-positron plasma which is produced is in the strong magnetic field of the neutron star. The magnetosphere fills a large volume, stretching out to distances $r \sim c/\Omega$, which are 10^3–10^4 times greater than the radius of the neutron star, R.

The plasma filling the magnetosphere screens the longitudinal electric field, and it begins to rotate along with the star as a rigid body. A corotation of this sort is indeed observed in the magnetospheres of planets: the earth and Jupiter. The plasma filling the magnetosphere becomes polar-

ized: A corotation charge forms with a density (Goldreich and Julian[38])

$$\rho_c = -\frac{(\Omega \mathbf{B})}{2\pi c}, \quad n_c = \frac{\rho_c}{e} = \frac{(\Omega \mathbf{B})}{2\pi c e}; \tag{2.2}$$

here e is the electron charge. In the earth's magnetosphere, for example, the density is $n_c \sim 10^{-6}$ particles/cm^3, while in the magnetosphere of a pulsar the density n_c reaches 10^{11}–10^{14} particles/cm^3. The rotation, i.e., the motion of the charge ρ_c, gives rise to electric currents. The maximum corotation current density is

$$j_c = c\rho_c = -\frac{(\Omega \mathbf{B})}{2\pi}. \tag{2.3}$$

The currents become deformed and perturb the magnetic field of the neutron star. While these perturbations are slight near the star, they become large and even governing factors at large distances from the star, $r \sim c/\Omega$. Because of the currents, the remote magnetic lines of force become stretched out and ultimately break. The situation is illustrated by Fig. 4. Two very different groups of lines of force thus form in the magnetosphere. One group consists of closed lines of force, i.e., lines of force which return to the surface of the star; the other group consists of open lines of force, which go off to infinity. The open lines emerge from small regions near the magnetic poles of the star—polar caps, with a radius

$$R_0 \approx R\left(\frac{\Omega R}{c}\right)^{1/2} \ll R. \tag{2.4}$$

Plasma can freely escape from the star along open lines of force. As it escapes, the charge ρ_c in (2.2) also escapes.

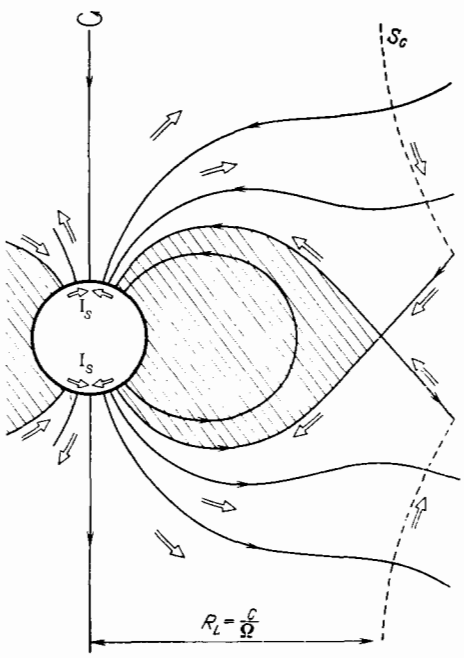

FIG. 4. Model of the current closure in the magnetosphere of a pulsar. At the light surface, S_c (the dashed lines), there is an additional acceleration of secondary plasma. The star is slowed down by the Ampère force which results from the surface current I_S, which closes the circuit for the longitudinal currents flowing in the magnetosphere. The hatching shows the region of closed lines of force.

However, the condition for screening and corotation will then be disrupted near the polar caps, with the result that a vacuum region appears, in which there is a strong potential electric field $E \sim E_{c0}(\Omega R/c)^{1/2}$. The potential difference across distances comparable to the size of the polar cap, (2.4), can reach $|\Psi_M| \approx E_{c0} R_0 (\Omega R/c)^{1/2}$:

$$\Psi_M \approx \left(\frac{\Delta R}{c}\right)^{3/2} R_0 B_0 \sim 10^{13} - 10^{15}\ \text{V}. \tag{2.5}$$

Under these conditions, as we have already mentioned, the vacuum is unstable: An electron-positron plasma is produced in it. The mechanism for this plasma production can be outlined as follows. The electric field—$\nabla\Psi$ which arises near the neutron star accelerates certain particles (the positrons, say) away from the star and others (the electrons) toward the star; which particles go toward and which away from the star depend on the sign of the charge ρ_c in (2.2). The particles move along a very strong magnetic field. Since the magnetic field is curvilinear, the particles which have acquired sufficient energy $\varepsilon \sim e\Psi_M$ begin to emit high-energy "curvature-radiation" [1)] photons: γ quanta. These γ photons are emitted along the direction in which the particle is moving, i.e., along the magnetic line of force. Since the magnetic field is curvilinear, however, the γ photon begins to move across it, and it eventually reaches the critical angle for the production of an electron-positron pair. This angle depends on the energy of the γ photon and the magnetic field strength. The particles of the other sign go through the same process, as they move through the electric field in the opposite direction. These particles also emit curvature radiation γ quanta, which produce pairs. The process of acceleration and pair production is then repeated. The result is a chain reaction in which there is a multiplication of electrons, positrons, and γ quanta near the neutron star. The multiplication coefficient increases because the particles produced at high Landau levels in the magnetic field emit synchrotron radiation: synchrotron photons, which are also capable of producing pairs.

As a result, a plasma is produced with a density three to five orders of magnitude greater than n_c in (2.2). This plasma moves away from the star at a velocity close to c and contains a broad distribution of particle energies ε. The maximum of the energy distribution typically falls at a Lorentz factor[44] $\gamma \sim \gamma_{\min} \approx \varepsilon/mc^2 \sim 300$–$500$. At $\gamma < \gamma_{\min}$ the distribution function is cut off sharply. All the relativistic particles with energies $\gamma \sim 100$–1000 moving the curvilinear magnetic field of the pulsar produce curvature radiation in the radio-frequency range 0.01–10 GHz, which is similar to ordinary synchrotron radiation. An important point, however, is that the wavelength of this radiation, λ_r, is many orders of magnitude greater than the mean distance between particles, and its phase velocity is close to the velocity of the particles. A strong collective interaction of waves and particles arises and gives rise to a Cherenkov radiation of rapidly growing hydrodynamic curvature-plasma modes. At a distance (10–100)R from the neutron star, these modes convert into ordinary radio waves. As a result, an intense flux of directed radio waves is produced at frequencies 0.01–10 GHz and is directed away from regions near the magnetic poles of the

pulsar. This picture is entirely in accordance with the generally accepted model for the emission of a pulsar (Fig. 1).

A steady-state production of plasma occurs near a pulsar only if the drop in the electric potential between the surface of the neutron star and the magnetosphere reaches a certain level $\Psi_c < |\Psi_M|$, which depends on the pulsar period P, the magnetic field B_0, and the radius of curvature of the magnetic line of force, ρ (Ref. 42). The value of the potential is typically $\Psi_c \sim 10^{13}$ V and depends relatively weakly on the properties of the surface of the neutron star. Since the potential Ψ_M always has a completely definite sign, which is the same as the sign of the charge ρ_c in (2.2), only charges of the same sign will be accelerated away from the surface of the star. The process by which the electron-positron plasma is produced is therefore always accompanied by the flow of an electric current with a density of the order of j_c in (2.3) along the magnetic lines of force. The total current I which drains from the star is of the order of I_c, given by

$$I_c \approx \pi R_0^2 j_c. \tag{2.6}$$

The total potential difference traversed by the current I is Ψ_M, given in (2.5). The power associated with this current is therefore

$$W = I\Psi_M; \tag{2.7}$$

this power is dissipated in the magnetosphere in the course of the production and acceleration of the electron-positron plasma, the γ quanta, and the radio waves.

Because of the potential drop Ψ_c between the surface of the star and the magnetosphere, the electric field in the magnetosphere near broken lines of force is not the same as the corotation field. The plasma in this part of the magnetosphere is not rotating as a rigid body along with the star; its rotation velocity becomes smaller.

The longitudinal current in the magnetosphere is flowing in the same direction over an entire polar cap. For this situation to be possible, there must exist a return current at the surface of the pulsar. This current closure occurs as is shown in Fig. 4. Near the light surface S_c, where the revolution velocity of the plasma particles approaches the velocity of light, the state of uniform rotation is disrupted, and particles begin to move across the magnetic lines of force. They are accelerated to energies $\varepsilon \sim 10^{10}$–10^{13} eV; the electrons and positrons are accelerated in different directions. As a result, an intense jet of an electric current forms along the light surface and flows in the direction across the magnetic lines of force. When this jet reaches the boundary of the closed magnetosphere, it continues to move along the separatrix separating the regions of open and closed lines of force, thereby returning to the surface of the neutron star.

As Fig. 4 shows, the current jet I_S then begins to flow along the surface of the star, crossing magnetic lines of force. A ponderomotive Ampère force $F_A = (1/c) I_S B_0$ arises and slows the rotation of the star. The slowing down of a neutron star is thus caused by the surface current. The energy of this slowing is released in part by the longitudinal current at the surface of the star ($I\Psi_c$), while the rest is expended on accelerating the electrons and positrons near the light surface.

The physical basis of the entire complex of processes which arise in the magnetosphere of a pulsar is therefore exceedingly simple and natural: Eveything happens as a result of the rapid rotation in vacuum of a highly magnetized conducting object: a neutron star. The rotation creates an electric field, which, in the presence of the strong, curvilinear magnetic field of the star, causes an effective production of an electron-positron plasma, i.e., the formation of a magnetosphere. The plasma in the magnetosphere of the rotating star reaches a state of corotation; corotation currents arise; and because of these currents some of the magnetic lines of force break and go off to infinity. Plasma escapes from the star along these lines of force, so that plasma must be produced continuously near the magnetic poles. This is the reason for the constant activity near the magnetic poles, which leads in particular to the appearance of the intense and directed radio emission of a pulsar. The energetics of all the processes is based on the slowing of the rotation of the star, caused by electric currents. The main role in the production and maintenance of the activity of a pulsar is played by the longitudinal current I which is circulating in the magnetosphere. The roles played by the surrounding medium and the particular structural features of the surface of the object are minor. In this sense, the theory which we will be examining below is physically closed and contains essentially no further assumptions of a model nature.

3. ELECTRODYNAMICS OF THE MAGNETOSPHERE

3.1. Basic equations. The electrodynamics of the magnetosphere of a pulsar is determined by the interaction of the electron-positron plasma with the magnetic field of the rotating neutron star. It is described by Maxwell's equations for the electric field $\mathbf{E}$ and the magnetic field $\mathbf{B}$ and by the kinetic equations for the distribution functions of electrons (F^-) and positrons (F^+):

$$\operatorname{div}\mathbf{E} = 4\pi\rho_e, \qquad \operatorname{rot}\mathbf{E} = -\frac{1}{c}\frac{\partial \mathbf{B}}{\partial t}, \tag{3.1}$$

$$\operatorname{rot}\mathbf{B} = \frac{4\pi}{c}\mathbf{j} + \frac{1}{c}\frac{\partial \mathbf{E}}{\partial t}, \quad \operatorname{div}\mathbf{B} = 0, \tag{3.2}$$

$$\frac{\partial F^{\pm}}{\partial t} - Bv_{\parallel}\frac{\partial}{\partial r_{\parallel}}\left(\frac{F^{\pm}}{B}\right) \pm \frac{e}{B}(\mathbf{EB})\frac{\partial F^{\pm}}{\partial p_{\parallel}} + \mathbf{v}_{\perp}\frac{\partial F^{\pm}}{\partial \mathbf{r}_{\perp}} = q, \tag{3.3}$$

$$\rho_e = e(n^+ - n^-); \qquad \mathbf{j} = e(n^+\mathbf{v}^+ - n^-\mathbf{v}^-); \tag{3.4}$$

here $r_{\parallel}$, $v_{\parallel}$, and $p_{\parallel}$ are the coordinate, velocity, and momentum of a particle along a magnetic line of force; $\mathbf{r}_{\perp}$, $\mathbf{v}_{\perp}$, and $\mathbf{p}_{\perp}$ are the same, but across the line of force; $F^{\pm}(p_{\parallel}, \mathbf{r}, t)$ is the distribution function of electrons or positrons with respect to the longitudinal momentum; $n^{\pm}$ and $\mathbf{v}^{\pm}$ are the densities and average velocities of the particles; and $q(p_{\parallel}, \mathbf{r}, t)$ is the density of the source of electron-positron pairs. We have taken into account the circumstance that the spread in transverse momentum $\mathbf{p}_{\perp}$ is negligible, because of both the particular way in which the electron-positron plasma is produced and the rapid synchrotron radiation, due to the large value of the magnetic field B_0. We thus have

$$F^{\pm}(p_{\perp}, \mathbf{p}_{\perp}, \mathbf{r}, t) = F^{\pm}(p_{\parallel}, \mathbf{r}, t)\,\delta(\mathbf{p}_{\perp} - \mathbf{p}_{\perp}^{\pm}(\mathbf{r}, t)),$$

where the functions $\mathbf{p}_{\perp}^{\pm}(\mathbf{r}, t)$ are determined by the equations

$$\left.\begin{aligned}&\frac{\partial \mathbf{p}_\perp^\pm}{\partial t}+(\mathbf{v}\nabla)\,\mathbf{p}_\perp^\pm \mp e\left(\mathbf{E}_\perp+\frac{1}{mc\gamma}[\mathbf{p}_\perp^\pm \mathbf{B}]\right)=0,\\ &\mathbf{p}_\perp=m\mathbf{v}_\perp\gamma,\quad \gamma=[1+(p_\parallel^2+p_\perp^2)\,m^{-2}c^{-2}]^{1/2},\\ &n^\pm=\int F^\pm\,\mathrm{d}p_\parallel,\quad n^\pm v_\parallel^\pm=\frac{1}{m}\int\frac{p_\parallel}{\gamma}F^\pm\,\mathrm{d}p_\parallel;\end{aligned}\right\}\tag{3.5}$$

here m is the rest mass of an electron, and γ is the Lorentz factor.

The initial equations can be simplified substantially. We first consider the steady-state solution. In the case of a star in uniform rotation, the steady-state solution depends on the time t and the azimuthal angle φ in the combination $\varphi-\Omega t$. We can therefore eliminate the time t from the equations, by using the substitution $\varphi'=\varphi-\Omega t$. As a result, Eqs. (3.1) and (3.2) acquire the steady-state form

$$\mathbf{E}=-[\boldsymbol{\beta}_\mathrm{R}\mathbf{B}]-\nabla\Psi;\tag{3.6}$$

$$\mathrm{rot}\,\mathbf{B}=\frac{4\pi}{c}\mathbf{j}-[\boldsymbol{\beta}_\mathrm{R}\,\mathrm{rot}\,[\boldsymbol{\beta}_\mathrm{R}\mathbf{B}]]+\nabla(\boldsymbol{\beta}_\mathrm{R}\nabla\Psi),\tag{3.7}$$

where $\boldsymbol{\beta}_R\equiv[\boldsymbol{\Omega}\mathbf{r}]/c$. The first term in (3.6) is the corotation electric field [cf. (2.1)], and Ψ is the electric potential in a frame of reference which is rotating at an angular velocity Ω. The potential Ψ shows the extent to which the actual field determining the motion of the plasma in the magnetosphere of the pulsar differs from the field of an exact corotation. It reflects the interaction of the magnetic field and the currents with the plasma and is the most important characteristic of the magnetosphere.

Furthermore, as we mentioned in §2 (see §4 for more details), the electron-positron plasma is produced by a source q in (3.3) in the immediate vicinity of the neutron star and then moves away from the star at a velocity close to c, along broken lines of force. The plasma density n_e in the magnetosphere always satisfies the condition

$$n_\mathrm{c}\ll n_\mathrm{e}\ll n_\mathrm{B};\tag{3.8}$$

here n_c is the corotation density, given by (2.2), and $n_B=B^2/8\pi\langle E\rangle$, where $\langle E\rangle$ is the average energy of the plasma particles. The condition $n_c<n_e$ means that the polarization of the plasma caused by the rotation leads to only a slight charge separation: $|n^+-n^-|/n_e\ll 1$ (if this condition does not hold, the charges become completely separated, and the medium is no longer a plasma). Because of the plasma polarization, the longitudinal electric field $E_\parallel$ is screened in the magnetosphere. Specifically, in the zeroth approximation in the parameter $1/\lambda$, where

$$\lambda=\frac{n_\mathrm{e}}{n_\mathrm{c}},\tag{3.9}$$

we can set $E_\parallel=0$, i.e., $\Psi=\Psi(\mathbf{r}_\perp)$.

The condition $n_e\ll n_B$ means that the energy density of the plasma is much smaller than that of the magnetic field. In the zeroth approximation in the parameter

$$\mu=\frac{n_\mathrm{e}}{n_\mathrm{B}}\ll 1\tag{3.10}$$

we can ignore the plasma pressure. In this case the transverse electric current is determined exclusively by the drift of the electric charge ρ_e in (3.1), so that the total current can be written

$$\mathbf{j}=c\rho_\mathrm{e}\frac{[\mathbf{EB}]}{B^2}+i\mathbf{B}\equiv c\rho_\mathrm{e}\boldsymbol{\beta}_\mathrm{R}-c\rho_\mathrm{e}\frac{[\nabla\Psi\mathbf{B}]}{B^2}+i_\parallel\mathbf{B}.\tag{3.11}$$

Using (3.1) and (3.6), we can then eliminate the charge density ρ_e and write the system of steady-state equations (3.7), (3.11), (3.3) in the following form[40]:

$$\begin{aligned}&\mathrm{rot}\,\{\mathbf{B}(1-\beta_\mathrm{R}^2)+\boldsymbol{\beta}_\mathrm{R}(\mathbf{B}\boldsymbol{\beta}_\mathrm{R})+[\boldsymbol{\beta}_\mathrm{R}\nabla\Psi]\}\\ &=\frac{4\pi}{1-\beta_\mathrm{R}^2+\beta_\mathrm{R}([\nabla\Psi\mathbf{B}]/B^2)}\left\{\frac{i_\parallel}{c}[(1-\beta_\mathrm{R}^2)\mathbf{B}+[\boldsymbol{\beta}_\mathrm{R}\nabla\Psi]]\right.\\ &\left.+\frac{[\nabla\Psi\mathbf{B}]}{B^2}\left[\frac{(\Omega\mathbf{B})}{2\pi c}+\frac{1}{4\pi}(\Delta\Psi-\boldsymbol{\beta}_\mathrm{R}\nabla(\boldsymbol{\beta}_\mathrm{R}\nabla\Psi))\right]\right\};\\ &\mathrm{div}\,\mathbf{B}=0,\\ &\Psi=\Psi(\mathbf{r}_\perp),\qquad \boldsymbol{\beta}_\mathrm{R}=[\boldsymbol{\Omega}\mathbf{r}]/c.\end{aligned}\tag{3.12}$$

The system of equations (3.12) is the final form. It describes the magnetic field configuration in the magnetosphere of a pulsar with an arbitrary electric field—$\nabla\psi$ and a longitudinal current $i_\parallel$. The two latter quantities serve as sources in Eqs. (3.12); they are determined by the conditions at the boundaries of the magnetosphere.

The boundary conditions on Eqs. (3.12) are as follows. Near the surface of the star, at the lower boundary of the magnetosphere, $S=S_0(\mathbf{r})$, the magnetic field determined by internal sources is given:

$$\mathbf{B}|_{S_0}=\mathbf{B}_0(\mathbf{r}).\tag{3.13}$$

Also given here are the longitudinal currents which are flowing into the magnetosphere and out of it,

$$\mathbf{j}_\parallel|_{S_0}=i_\parallel(\mathbf{r}_\perp)\,\mathbf{B}_0,\tag{3.14}$$

and the electric potential,

$$\Psi|_{S_0}=\Psi(\mathbf{r}_\perp).\tag{3.15}$$

There are important differences between the region in which the closed magnetic lines of force emerge and the region in which the broken lines of force (i.e., those which go off to infinity) emerge (§2). If we assume the conductivity of the star to be infinite, we can assume that there are no longitudinal currents in the region of closed lines of force, $S_{c1}(\mathbf{r})$, and there is complete corotation:

$$i_\parallel|_{S_{c1}}=0,\qquad \Psi|_{S_{c1}}=0.\tag{3.16}$$

Boundary conditions (3.14) and (3.15) are thus of a nontrivial nature and lead to a substantial change in the form of the equations only in the region of open lines of force.

Yet another natural condition arises at the surface S_d defined by the relation

$$1-\beta_\mathrm{R}^2+\boldsymbol{\beta}_\mathrm{R}\frac{[\nabla\Psi\mathbf{B}]}{B^2}=0.\tag{3.17}$$

The right side of Eqs. (3.12) has a singularity at this surface. The requirement that the magnetic lines of force must be able to intersect the singular surface S_d, i.e., that the electric charge ρ_e and the current $\mathbf{j}$ must remain finite at this surface, is a natural boundary condition of the problem. Finally, we need to require that all the fields vanish at infinity.

We wish to emphasize that near the "light surface" S_c, where $E\to B$, the particle drift velocity approaches the velocity of light. There is accordingly an increase in the energy of the particles here, and there is a corresponding sharp increase in the expansion parameter μ in (3.10). As a result,

the conditions for the applicability of Eq. (3.12) are violated near S_c. A singular boundary layer forms here, in which approximation (3.11) is no longer sufficient, and a more accurate solution of equations of motion (3.5) is necessary. The surface S_c is therefore a sort of boundary of the magnetosphere, outside which Eqs. (3.12) do not hold. However, the additional requirement that the fields vanish at infinity is correct, since the range of applicability of approximation (3.11) along the rotation axis extends without bound.

3.2. Axisymmetric case. We begin with the simplest case. We assume that the unperturbed magnetic field of the pulsar is a dipole field, with dipole axis running parallel to the rotation axis. In this case, the magnetic field can be written in the cylindrical coordinates $\rho_\perp, \varphi, z$ (the z axis is along the rotation axis) as follows:

$$\mathbf{B} = \frac{1}{\rho_\perp}[\nabla f \mathbf{e}_\varphi] + \frac{g}{\rho_\perp}\mathbf{e}_\varphi,$$

where the scalar function $f(\rho_\perp, z)$ does not depend on the azimuthal angle φ. Since we have $(\mathbf{B}\nabla f) = 0$, the function $f(\rho_\perp, z)$ is constant along the magnetic lines of force, so that the condition $E_\parallel = 0$ can be rewritten as

$$\Psi = \Psi(f). \tag{3.18}$$

Finally, the function $g(\rho_\perp, z)$ is related to the longitudinal current $i_\parallel$ which flows in the magnetosphere, as is easily verified. By virtue of our basic equation (3.12), we have $g = g(f)$, in the axisymmetric case, so that at the surface of the star we have

$$\frac{4\pi}{c} i_\parallel = \frac{dg}{df}. \tag{3.19}$$

Finally, Eq. (3.12) reduces to a single nonlinear equation for the scalar function $f(\rho_\perp, z)$:

$$-\Delta f\left[1 - \frac{\Omega^2\rho_\perp^2}{c^2}\left(1 + \frac{\Omega}{c}\frac{d\Psi}{df}\right)^2\right] + \frac{2}{\rho_\perp}\frac{\partial f}{\partial \rho_\perp} - g\frac{dg}{df}$$
$$+ \frac{\Omega^3\rho_\perp^2}{c^3}\left(1 + \frac{\Omega}{c}\frac{d\Psi}{df}\right)\frac{d^2\Psi}{df^2}(\nabla f)^2 = 0. \tag{3.20}$$

The functions $\Psi(f)$ and $g(f)$, determined by boundary conditions (3.14)–(3.16), serve as sources in Eq. (3.20).

If there is no electric field or longitudinal current anywhere in the magnetosphere, conditions (3.16) hold on both the closed and open lines of force: $\Psi(f) = 0$ and $g(f) = 0$. Equation (3.2) takes the simple form

$$-\Delta f\left(1 - \frac{\Omega^2\rho_\perp^2}{c^2}\right) + \frac{2}{\rho_\perp}\frac{\partial f}{\partial \rho_\perp} = 0. \tag{3.21}$$

Figure 5 shows the solution of Eq. (3.21) found numerically by Michel[49] and Mestel and Wang.[50] We see that the light surface S_c is a cylinder of radius c/Ω, as it should be, since in this case corotation prevails throughout the magnetosphere. At $f > f^*$ the magnetic lines of force are closed and do not reach the singular surface S_c; at $f < f^*$ they are open; i.e., they intersect the singular surface S_c and go off to infinity. Here we have $f^* = 1.592M\Omega/c$, where M is the magnetic moment of the star. At the intersection of the separatrix $f = f^*$ and the light cylinder there is a magnetic null line.

We turn now to the solution of the main problem: incorporating the longitudinal currents $i_\parallel$ and the electric field Ψ in the region of open lines of force, i.e., at $f < f^*$. Equation

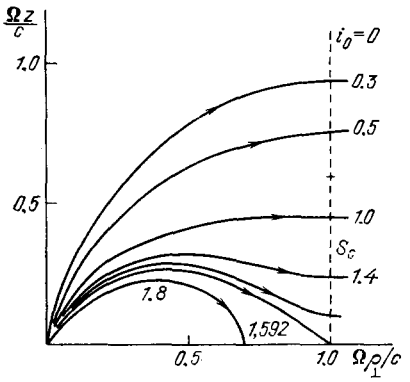

FIG. 5. Magnetic lines of force ($f = \text{const}$) in the absence of a longitudinal current i_0 and of an accelerating potential β_0 (Refs. 49 and 50). Here S_c is the light surface, which in this case coincides with the light cylinder (the numbers are the values of $fc/M\Omega$).

(3.20) simplifies substantially in this case if we choose the source functions in (3.14) and (3.15) to be

$$\Psi(f) = \frac{\Omega}{c}\beta_0(f^* - f), \quad g(f) = \frac{4\pi\Omega}{c} i_0 f, \quad f < f^*, \tag{3.22}$$
$$\Psi(f) = 0, \qquad g(f) = 0, \qquad f > f^*;$$

where i_0 and β_0 are dimensionless parameters; i_0 is the density of the longitudinal current $j_\parallel$ expressed in units of the current $2j_c$ in (2.3), and β_0 is the drop in the potential Ψ_c expressed in units of Ψ_M in (2.5).

Equation (3.20) in the region $f < f^*$ can be rewritten as

$$\Delta f\left[1 - \frac{\Omega^2\rho_\perp^2}{c^2}(1-\beta_0)^2\right] - \frac{2}{\rho_\perp}\frac{\partial f}{\partial \rho_\perp}$$
$$+ \frac{\Omega^2}{c^2} i_0^2 f = 0. \tag{3.23}$$

In the region $f > f^*$, the equation remains of the same form as in (3.21).

Boundary conditions (3.22) correspond to the following picture of the currents in the magnetosphere of a pulsar: The density of the flowing current i_0 is constant over the entire region of open lines of force, while the return current forms an intense current jet [a discontinuity in the function $g(f)$ near the boundary $f = f^*$. When there is a longitudinal current ($i_0 \neq 0$) and a field $\Psi(\beta_0 \neq 0)$, we should thus seek a solution of Eq. (3.23) at $f < f^*$ and join it with the solution of Eq. (3.21) at $f > f^*$. A joining of this sort would be possible, however, only if the "compatibility relation"[40]

$$\beta_0 = 1 - \left(1 - \frac{i_0^2}{i_M^2}\right)^{1/2}, \qquad i_M^2 = \frac{c^2}{\Omega^2}\frac{|\Delta f|}{f^*}\Big|_{z=0,\ \rho_\perp = c/\Omega} \approx 1{,}57, \tag{3.24}$$

which relates i_0 and β_0, holds. Additional relation (3.24) has to be introduced because of the nonlinearity of Eq. (3.20), which describes the entire magnetosphere of the pulsar.

Figure 6 shows an example of a solution constructed in this way. The dashed lines show the singular surface S_d and the light surface S_c. We see that the surface S_c lies beyond the light cylinder, $\Omega\rho_\perp/c = 1$. This result means that the

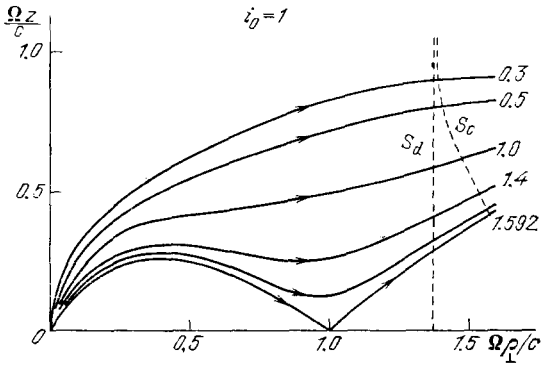

FIG. 6. Magnetic field configuration in the presence of a longitudinal current ($i_0 = 1$). The dashed lines show the light surface S_c and the singular surface S_d.

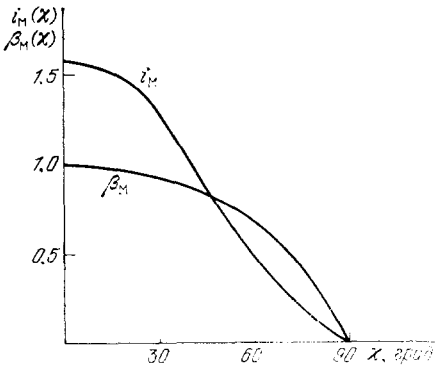

FIG. 7. The quantities $i_M^2(\chi)$ and $\beta_M(\chi)$, which appear in "compatibility relation" (3.25), as functions of the angle χ.

rotation of the magnetosphere has slowed down substantially. The magnetosphere remains divided into regions of open and closed lines of force, and the null line is at $\rho_\perp = c/\Omega$, $z = 0$.

We wish to emphasize the importance of compatibility relation (3.24), which relates the flowing longitudinal current i_0 to the electric field β_0 or the drop in the potential between the surface of the star and the magnetosphere, $\Psi(f)$, given by (3.22). This relation serves as a nonlinear Ohm's law, and it determines the energy loss of the pulsar, as we will see. Furthermore, it follows from (3.24) that the density of the longitudinal current i_0 cannot exceed the critical value i_M. It turns out that in order to derive compatibility relation (3.24) we need to know only the behavior of the solution of (3.21) ($i_0 = 0$, $\beta_0 = 0$) near the magnetic null line. Relation (3.24) follows from Eq. (3.23), since near the null line ($\Omega\rho_\perp/c = 1, f = f^*$) the magnetic field is weak, so that we have $\nabla f \to 0$.

This remarkable fact makes it possible to derive a compatibility relation for an arbitrary inclination of the axis of the magnetic dipole with respect to the rotation axis χ. This relation is

$$\beta_0 = \beta_M(\chi)\left[1 - \left(1 - \frac{i_0^2}{i_M^2(\chi)}\right)^{1/2}\right] \qquad (3.25)$$

and is completely analogous to (3.24). The only changes are in the coefficients $\beta_M(\chi)$ and $i_M(\chi)$, which are shown in Fig. 7. Figure 8 shows the structure of the magnetosphere for axis inclination angles $\chi = 30°$ and 90°. We will not discuss the case of inclined axes in more detail here (see Ref. 40).

3.3. Boundary layer; current closure. The solutions constructed above are valid only up to the light surface, where the total electric field E is comparable in magnitude to the magnetic field B. Here the particle drift velocity approaches the velocity of light, and the energy of the particles increases sharply; condition (3.10) breaks down. A singular boundary layer thus forms near the light surface. In it, drift approximation (3.11) is inadequate, and we need a more accurate description of the motion of the electrons and positrons.

As we will see, the thickness of the boundary layer at $n_e \gg n_c$ in (3.8) is always small in comparison with the dimensions of the magnetosphere. In the steady state, all quantities in this layer thus vary substantially only in the direction normal to the layer, $\rho_\perp$. Making use of this circumstance, we rewrite the basic equations, (3.1), (3.2), (3.6), as

$$\frac{\partial B_\varphi}{\partial \rho_\perp} = \frac{4\pi}{c} j_z, \quad \frac{\partial B_z}{\partial \rho_\perp} = -\frac{4\pi}{c} j_\varphi, \quad \frac{\partial}{\partial \rho_\perp}(\rho_\perp B_{\rho_\perp}) = 0,$$
$$\frac{\partial^2 \Psi}{\partial \rho_\perp^2} = -2\frac{\Omega B_z}{c} + 4\pi\left(\frac{\Omega \rho_\perp}{c^2} j_\varphi - \rho_e\right) \qquad (3.26)$$

The distribution of electrons and positrons is described by kinetic equations (3.3)–(3.5), where $q = 0$. Near the light surface, the particles are accelerated to a great extent, so that their initial spread in longitudinal momentum can be ignored. Now writing the particle distribution function as

$$F^\pm = n^\pm(\rho_\perp)\,\delta[\mathbf{p} - \mathbf{p}^\pm(\rho_\perp)], \qquad (3.27)$$

we find from (3.4) and (3.5)

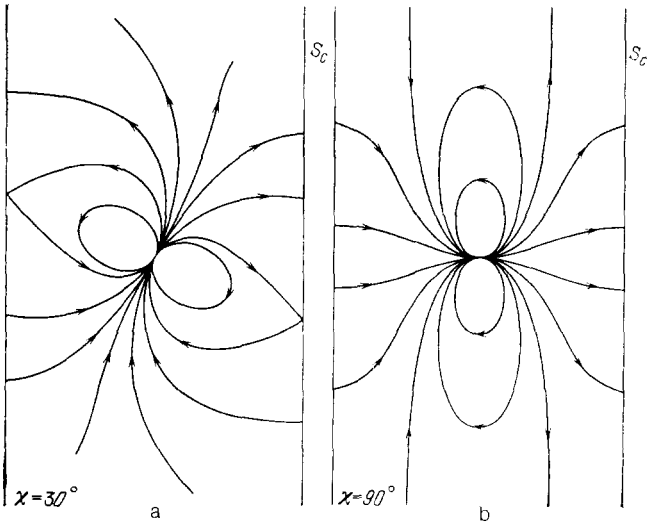

FIG. 8. Structure of the magnetosphere of a pulsar for axis inclination angles $\chi = 30°$ and 90°. Here S_c is the light surface, which coincides with the light cylinder in the case $i_0 = 0$.

$$\left.\begin{aligned}
&\frac{d}{d\rho_\perp}\left(\frac{p_{\rho_\perp}^{\pm} n^{\pm}}{\gamma^{\pm}}\right)=0;\\
&\frac{dp_{\rho_\perp}^{\pm}}{d\rho_\perp}=\frac{p_\varphi^{\pm 2}}{\rho_\perp p_{\rho_\perp}^{\pm}}\pm\frac{e\gamma^{\pm}}{p_{\rho_\perp}^{\pm}}\left(mE_{\rho_\perp}+\frac{1}{c\gamma^{\pm}}[\mathbf{p}^{\pm}\mathbf{B}]_{\rho_\perp}\right);\\
&\frac{dp_\varphi^{\pm}}{d\rho_\perp}=-\frac{p_\varphi^{\pm}}{\rho_\perp}\pm\frac{e\gamma^{\pm}}{p_{\rho_\perp}^{\pm}}\left(mE_\varphi+\frac{1}{c\gamma^{\pm}}[\mathbf{p}^{\pm}\mathbf{B}]_\varphi\right),\\
&\frac{dp_z^{\pm}}{d\rho_\perp}=\pm\frac{e\gamma^{\pm}}{p_{\rho_\perp}^{\pm}}\left(mE_z+\frac{1}{c\gamma^{\pm}}[\mathbf{p}^{\pm}\mathbf{B}]_z\right).
\end{aligned}\right\}\quad(3.28)$$

Equations (3.26)–(3.28) constitute a complete system of equations describing the distribution of the plasma and the field in the boundary layer.

Figure 9 shows the solution of these equations. Here s is the distance from the light surface, in units of $(c/4\pi\lambda\Omega)I/I_c$, where $\lambda=n_e/n_c$ in (3.9). By virtue of condition (3.8), the condition $\lambda>1$ always holds, so that the boundary layer is thin. Specifically, its thickness $\Delta\rho_\perp\sim c/\Omega\lambda$ is much smaller than the scale of the magnetosphere, $r\sim c/\Omega$. It can be seen from Fig. 9 that the energy of the electrons and the positrons in the boundary layer increases to $\varepsilon\sim\varepsilon_M$, where

$$\varepsilon_M=\frac{eI}{c\lambda}=\frac{eB_0\Omega^2R^3}{\lambda c^2}\,i_0. \quad (3.29)$$

It follows that the maximum energy of the particles is proportional to the total current I circulating in the magnetosphere and inversely proportional to the particle density. The total particle density becomes comparable to the energy density of the electromagnetic field at $s\sim 1$. As a result, the condition $\mu<1$ [see (3.10) and (3.8)] is violated, so that the properties of the medium change substantially: The Alfvén velocity becomes comparable to the velocity of light, and excitation of magnetosonic waves becomes possible. The particles escape into the region $s>2$ along with the MHD radiation; their average energy remains of the order of ε_M.

The momentum in the rotation direction, p_φ, increases in proportion to the energy. The momentum in the radial direction, $p_{\rho_\perp}$, has a more distinctive behavior in the boundary layer. As we see from the figure, it initially increases and then decreases, resulting in an accumulation of particles in the layer. The motion of the particles in the z direction, parallel to the light surface, is substantial only in the boundary layer, as we see from the figure. The momentum p_z increases most rapidly. The primary feature here is that the particles with charges of different sign move in opposite directions along z. This result means that a strong electric current arises in the thin boundary layer (Fig. 4). A jet of surface current, flowing in the z direction, i.e., along the light surface, forms. The intensity of the current jet is

$$I_{S_c}=-\frac{1}{4\pi}B_\varphi^{(0)}c; \quad (3.30)$$

here $B_\varphi^{(0)}=i_0B_0(\Omega R/c)^3$ is the azimuthal component of the magnetic field at the boundary of the layer, i.e., at $s=0$. Because of the intense surface current I_{S_c} in (3.30), the component B_φ decreases rapidly in the boundary layer, as can be seen from Fig. 9. The vanishing of B_φ at $s=\sqrt{3}$ corresponds to complete closure by the current jet in the boundary layer of the longitudinal currents which are flowing in the magnetosphere (Fig. 4).

As the separatrix is approached, $f\to f^*$, the potential difference between the surface of the star and the magnetosphere vanishes, as can be seen from (3.22). The current becomes able to return freely to the surface of the star. Where the light surface intersects the light line $f=f^*$, the current jet thus turns, and returns to the surface of the pulsar along the separatrix $f=f^*$ (Fig. 4). This result is in complete accordance with conditions (3.22): The discontinuity in $g(f)$ at $f=f^*$ means that there is a return-current jet. Its magnitude is

$$I_j=-\frac{\Omega}{2\pi c}I. \quad (3.31)$$

This jet completely compensates for the forward longitudinal current I which flows throughout the magnetosphere of the pulsar. In this manner, there is a circulation of the current in the magnetosphere of the pulsar.

3.4. Energy loss of a pulsar. Let us determine the loss of rotational energy of a pulsar. The slowing of the star results from the current $\mathbf{I}_S$ which is flowing along the surface of the star, S. The moment of forces acting on the star is

$$\mathbf{K}=\frac{1}{c}\int[\mathbf{r}[\mathbf{I}_S\mathbf{B}_0(S)]]\,dS; \quad (3.32)$$

here $\mathbf{B}_0(S)$ is the magnetic field at the surface of the star. The projection onto the rotation axis Ω determines the loss of kinetic energy of the pulsar:

$$\frac{dE_{kin}}{dt}=-W=\mathbf{K}\boldsymbol{\Omega}=I_r\Omega\dot{\Omega}; \quad (3.33)$$

here I_r is the moment of inertia of the star. The other components of the vector $\mathbf{K}$ determine the rotation of the rotation axis with respect to the magnetic moment of the star, $\mathbf{M}$; i.e., they change the axis inclination angle χ.

In finding the surface current $\mathbf{I}_S$ it is convenient to distinguish between the potential and solenoidal parts of this current.[51] The potential part is determined by the longitudi-

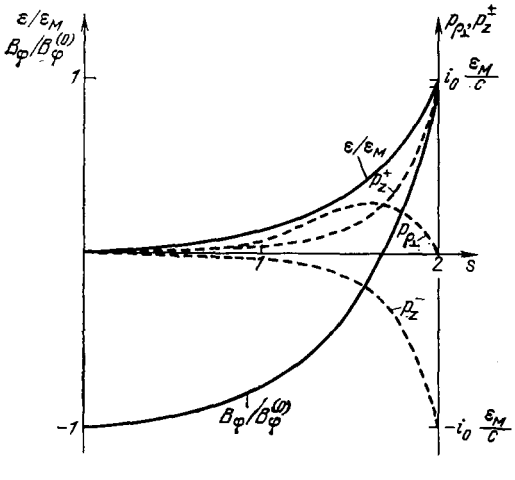

FIG. 9. Profiles of the energy ε and the momentum (the components $p_{\rho_\perp}$ and p_z) of the particles and also of the magnetic field B_φ in the boundary layer.

nal currents which drain into the magnetosphere from the surface of the star. It turns out that the retarding moment **K** is determined exclusively by the potential surface current, since it is proportional to the dimensionless density of the longitudinal current i_0 in (3.22):

$$\mathbf{K} = -L\frac{B_0^2\Omega^3R^6}{c^3}\,i_0\frac{\mathbf{M}}{M}\,; \tag{3.34}$$

here L is a numerical coefficient, approximately equal to[2] 0.4. It follows from (3.33) and (3.34) that in addition to the slowing, i.e., the decrease in the magnitude of the angular rotation velocity of the star,

$$\dot{\Omega} = -L\frac{B_0^2\Omega^3R^6}{c^3I_r}\,i_0\cos\chi, \tag{3.35}$$

there is also a regular increase in the axis inclination angle if the star is strictly spherically symmetric, as was pointed out by Heintzmann[52]:

$$\sin\chi = \frac{\Omega_0}{\Omega}\sin\chi_0, \qquad \dot{\chi} = -\frac{\dot{\Omega}}{\Omega}\operatorname{tg}\chi\,. \tag{3.36}$$

Here χ_0 and Ω_0 are the initial values of the inclination angle and of the angular velocity. We recall that the current i_0 is bounded in our case: $i_0 \leqslant i_M(\chi)$. The maximum current, i_M, depends strongly on the axis inclination angle χ (Fig. 7).

The energy carried off from the star, W, inside the light surface is the sum of two parts: the energy carried off by the flux of particles which are accelerated by the drop in the potential $\Psi(f)$ near the surface of the star (W_p) and the energy carried off by the electromagnetic field[40] (W_{em}):

$$\begin{aligned} W = W_p + W_{em} &= L\frac{B_0^2\Omega^4R^6}{c^3}\,i_0\cos\chi; \\ W_p &= L\frac{B_0^2\Omega^4R^6}{c^3}\,i_0\beta_0; \\ W_{em} &= L\frac{B_0^2\Omega^4R^6}{c^3}\,i_0(\cos\chi-\beta_0). \end{aligned} \tag{3.37}$$

We see that the flux of accelerated particles carries only part of the energy away from the pulsar, and this fraction is small if $\beta_0 < 1$ [or if $i_0 < 1$; see (3.24)]. However, in the boundary layer near the light surface the electrons and positrons of the entire plasma are accelerated, and they acquire an energy ε_M, given by (3.29). The electromagnetic energy flux W_{em} is entirely transferred to the plasma particles and to MHD waves. The total energy flux carried away from the star, W, is equal to the energy of the slowing of the star, given by (3.33) and (3.35). The energy flux W naturally is in accordance with estimate (2.7).

In the past, the slowing of a pulsar has usually been attributed to the loss of energy of a magnetic dipole which is rotating in a vacuum[25,53]:

$$W_d = \frac{1}{6}\frac{B_0^2\Omega^4R^6}{c^3}\sin^2\chi. \tag{3.38}$$

The dipole loss W_d is a vacuum loss; the current loss W in (3.37) arises when there is a plasma-filled magnetosphere. Comparison of W with W_d reveals that the primary distinction is the difference in the behavior as a function of the axis inclination angle: The dipole loss reaches a maximum when the axes are orthogonal, and it vanishes completely in the limit $\chi \to 0°$. The current loss, in contrast, is at a maximum in the axisymmetric case and decreases with increasing χ. This behavior of the current loss seems completely natural on physical grounds. The point is that the original cause of the loss is the need for plasma production on the open lines of force, and the amount of plasma, which is proportional to ρ_c, decreases with increasing angle χ [see (2.2)].

The most important distinction between the current loss and the dipole loss is that the former is proportional to the longitudinal current which drains away from the surface of the pulsar, as is reflected in (3.37) by the dimensionless factor.

$$i_0 = 2\cdot\cos\chi\,\frac{j_\parallel}{j_c}\,;$$

here $j_\parallel$ is the longitudinal current density, and j_c is the critical current, given by (2.3). The factor i_0 cannot exceed i_M in (3.25). As $i_0 \to i_M$, the current loss becomes comparable in magnitude to the dipole loss, while at $i_0 \ll i_M$ the current loss is much smaller. In particular, if there is no longitudinal current at all ($i_0 = 0$) a rotating star surrounded by a plasma magnetosphere loses no energy at all, regardless of the axis inclination angle χ. The physical reason is that in the absence of a longitudinal current the magnetospheric plasma becomes polarized in such a way that the radiation is completely suppressed. The Poynting vector in this case has only a component along φ on the light cylinder, so that the energy flux directed away from the star is zero.

An important point is that the longitudinal current i_0 is related to the electric potential Ψ by virtue of compatibility relation (3.24), (3.25). This potential, on the other hand, is determined by the conditions for the production of electron-positron pairs. Ultimately, therefore, it is the production of plasma on the open lines of force which determines the current i_0 and thus the slowing of the pulsar. We wish to stress that compatibility relation (3.25) leads immediately to the conclusion that a rotating neutron star becomes a radiopulsar only if an e^+e^- plasma is produced from vacuum near the star. Since we have $W \propto i_0 \approx (\Psi_0/\Psi_M)^{1/2}$ ($\Psi_M \gtrsim 10^{13}$ V), the loss of rotational energy of the star can be great enough to explain the observed radio emission only under the condition $\Psi_0 \gtrsim 10^9$–10^{10} V. Such large values of the potential drop near the surface of the star, Ψ_0, could arise only if the plasma is produced from vacuum.

4. PRODUCTION OF AN ELECTRON-POSITRON PLASMA

4.1. Basic equations. The plasma production mechanism suggested by Sturrock[43] and developed by Ruderman and Sutherland[54] and other investigators[42,44,55–59] involves an acceleration of electrons and positrons in a strong electric field near a neutron star and the emission of high-energy curvature γ photons by these particles as they move in a curvilinear magnetic field. The γ photons produce electron-positron pairs (§2). This process is described by the kinetic equations for the particles, (3.3), and for the γ photons, and by Maxwell's equations, (3.1) and (3.2), for the field. The initial equations simplify because the plasma production occurs close to the pulsar, at $(r - R) \lesssim R$, for the most part, so that the drift of the charged particles and perturbations of the magnetic field can be ignored. They accordingly take the form

$$\frac{\partial F_\sigma^\pm}{\partial t}+\sigma c\mathbf{B}\left\{\frac{\partial}{\partial \mathbf{r}}\left[\frac{(\gamma^2-1)^{1/2}}{\gamma B}F_\sigma^\pm\right]\right.$$

$$\left.\mp\frac{e\nabla\Psi}{mc^2B}\frac{\partial}{\partial\gamma}\left[\frac{(\gamma^2-1)^{1/2}}{\gamma}F_\sigma^\pm\right]\right\}=-D_1+q_G, \tag{4.1}$$

$$\frac{\partial G}{\partial t}+c\frac{\mathbf{k}}{k}\frac{\partial G}{\partial \mathbf{r}}=q_F+q_S-D, \tag{4.2}$$

$$\Delta\Psi=-4\pi e\left[\sum_\sigma\int_1^\infty(F_\sigma^+-F_\sigma^-)\,d\gamma-n_c\right]; \tag{4.3}$$

where $F_\sigma^\pm(\gamma,\mathbf{r},t)$ is the energy distribution of the positrons and electrons; $\gamma=[1+(p_\parallel/mc)^2]^{1/2}$ (we are using the relation $p_\perp\ll p_\parallel$); and the factor and index $\sigma=\operatorname{sign}(\mathbf{p}_\parallel\mathbf{B})=\mp1$ characterize the direction of the longitudinal momentum [the relationship between $p_\parallel$ and γ is multivalued, so that a single function $F(p_\parallel)$ corresponds to two functions $F_\sigma(\gamma)$]. The operator $D_1(F_\sigma^\pm)$ describes the scattering of electrons and positrons as they emit γ photons, while the operator q_G describes the production of electron-positron pairs by high-energy γ photons. The function $G(\mathbf{k},\mathbf{r},t)$ is the distribution function of the γ photons with respect to the momentum $\mathbf{k}$; the operator q_F describes the production of curvature γ photons by fast electrons and positrons; q_S describes the emission of synchrotron photons by particles in nonzero Λ levels; and D describes the loss of γ photons due to pair production. Finally, Ψ is the electric potential given by (3.6), and n_c is the corotation density, given by (2.2). In (4.3) we have taken into account the circumstance that Eqs. (3.1) and (3.6) reduce to a Poisson equation in a rotating coordinate system in the absence of magnetic perturbations.

We can write the specific expressions for the operators D_i, D, q_G, q_F, and q_S. The scattering operator is[42]

$$D_1(F)=-\frac{2}{3}\alpha_f\frac{c\lambda}{\rho^2}\frac{\partial}{\partial\gamma}\left[\gamma^4F+\frac{55}{32\sqrt{3}}\frac{\lambda}{\rho}\frac{\partial}{\partial\gamma}(\gamma^7F)\right]; \tag{4.4}$$

here $\alpha_f=e^2/\hbar c$ is the fine-structure constant, $\lambda=\hbar/mc$ is the Compton wavelength,

$$\rho=\frac{4}{3}\left(\frac{Rcf^*}{\Omega f}\right)^{1/2}\left(\frac{r}{R}\right)^{1/2}$$

$$\approx 7.5\cdot10^7P^{1/2}\left(\frac{f}{f^*}\right)^{-1/2}\left(\frac{r}{R}\right)^{1/2}\text{cm} \tag{4.5}$$

is the radius of curvature of the magnetic field along the given line of force, ρ in the numerical expression is given in centimeters, and P is given in seconds. The operator describing pair production by γ photons is

$$q_G=\int w_1(\mathbf{k})\,G(\mathbf{k})\,\delta\left(\gamma-\frac{1}{|\sin\theta|}\right)d\mathbf{k}, \tag{4.6}$$

where $w_1(\mathbf{k})$ is the probability for the single-photon production of a pair in the magnetic field B (Ref. 60):

$$w_1(\varkappa)=\frac{3\sqrt{3}}{16\sqrt{2}}\alpha_f\frac{c}{\lambda}B_\hbar|\sin\theta|$$

$$\times\exp\left(-\frac{8}{3\varkappa B_\hbar|\sin\theta|}\right)\Theta_1(\varkappa|\sin\theta|-2);$$

$$\cos\theta=\frac{\mathbf{kB}}{kB},\quad \Theta_1(x)=\begin{cases}1, & x>0,\\ 0, & x<0;\end{cases}$$

here and below, we are using the dimensionless wave number $\varkappa$ (in units of λ^{-1}; i.e., $\varkappa=\hbar\omega/mc^2$), and the dimensionless magnetic field is $B_\hbar=B/B_c$ ($B_c=m^2c^3/\hbar e=4.4\cdot10^{13}$ G is the critical magnetic field). The operator describing the production of curvature photons is

$$q_F=\int_1^\infty d\gamma\,[F_\sigma^+(\gamma)+F_\sigma^-(\gamma)]\int_0^\infty d\varkappa P_c(\varkappa,\gamma)\,\delta\left(\varkappa-\sigma\frac{\mathbf{B}}{B}\varkappa\right); \tag{4.7}$$

here $P_c(\varkappa,\gamma)d\varkappa$ is the probability for the emission of a curvature photon in the interval $d\varkappa$, given by[61]

$$P_c(\varkappa,\gamma)=\frac{\sqrt{3}}{2\pi}\alpha_f\frac{c}{\rho}\frac{\gamma}{\varkappa_c}\int_{\varkappa/\varkappa_c}^\infty K_{5/3}(x)\,dx,\quad \varkappa_c=\frac{3}{2}\frac{\lambda}{\rho}\gamma^3,$$

and $K_{5/3}(x)$ is the modified Hankel function. The operator describing the production of synchrotron photons is

$$q_S=\frac{3\sqrt{3}}{(2\pi)^2}\frac{1}{\varkappa^3B_\hbar|\sin\theta|}$$

$$\times\int\frac{w_1(\varkappa')\,G(\varkappa')\frac{\varkappa'}{\varkappa_B}\int_{\varkappa'/\varkappa_B}^\infty K_{5/3}(x)\,dx}{(\sin^2\theta'-\sin^2\theta)^{1/2}}$$

$$\times\Theta_1\left[\sin^2\theta'-\sin^2\theta-\frac{4\cos^2\theta}{\varkappa'^2}\right]d\varkappa',$$

$$\varkappa_B=\frac{3}{2}B_\hbar|\sin\theta|\cos^2\theta\,(\sin^2\theta'-\sin^2\theta)^{-1}. \tag{4.8}$$

Finally, the operator describing the loss of γ photons on pair production is

$$D=w_1(\varkappa)\,G(\varkappa). \tag{4.9}$$

The system (4.1)–(4.9) is valid under the conditions

$$B_\hbar\lesssim0.1,\quad \frac{\lambda\gamma^3}{\rho}\ll1,\quad \varkappa^2\ll\frac{\alpha_f\rho}{\lambda B_\hbar},$$

which are satisfied quite well in the magnetosphere of a pulsar (ordinarily, we would have $B_\hbar\sim0.01$–0.1, $\rho\sim10^8$ cm, $\gamma\sim10^7$, $\varkappa\sim10^4$).[3)]

The boundary conditions on Eqs. (4.1)–(4.3) are specified at the surface of the star, $h=0$, and at large values $h\gtrsim R$, where the plasma production process has essentially ended (h is the height above the surface of the star near the polar cap). At $h=0$ we have

$$F_1^\pm(\gamma,\,h=0)=K^\pm(F_{-1}^+,\,F_{-1}^-,\,G^{(-)})|_{h=0}+F_{1_0}^\pm,$$
$$G^{(+)}(\varkappa,\,h=0)=K_G(F_{-1}^+,\,F_{-1}^-,\,G^{(-)})|_{h=0}+G_0^{(+)}. \tag{4.10}$$

For definiteness we have assumed here that the vector $\mathbf{B}$ is directed away from the surface of the star. The functions $F_1^\pm$ and $G^{(+)}$ therefore correspond to particles and photons which are moving away from the surface, while $F_{-1}^\pm$ and $G^{(-)}$ correspond to those moving toward the surface. The coefficients $K^\pm$ and K_G describe the ejection of electrons, positrons, and γ photons with energies above 1 MeV away from the surface of the star by accelerated particles which are incident on this surface from the plasma. These operators are generally linear. The coefficients $F_{1_0}^\pm$ and $G_0^{(+)}$ describe the independent emission of the same particles from the surface due to other processes (thermionic emission and

cold emission caused by the electric field). At large distances $h \gtrsim R$, the plasma which is produced moves away from the star, i.e., we have

$$F^{\bullet}_{-1} = F^{-}_{-1} = G^{(-)} = 0, \qquad h \gg R. \tag{4.11}$$

In this case the electric potential tends toward the constant value Ψ_∞, determined by the quasineutrality condition

$$\int_1^\infty (F_1^+ - F_1^-)\, d\gamma = n_c (1 - i_0^2)^{1/2}. \tag{4.12}$$

Here we have used the fact that when there is a longitudinal current $i_0 = 2j/j_c$ the angular velocity of the rotation of the magnetospheric plasma decreases according to (3.24) and (3.25). Below we will reckon the plasma potential from Ψ_∞; i.e., we will set $\Psi_\infty = 0$.

4.2. Double layer; critical "breakdown" potential. The existence of a significant potential difference between the surface of the star and the magnetosphere, Ψ_c, leads to a natural distinction of a layer near the surface in which there is a strong electric field. This layer is analogous to an ordinary Langmuir double layer near the surface of an object in a plasma. We will accordingly call it a "double layer" ("vacuum gap" is frequently used in the literature on pulsars[54]). It is in this double layer that the particles acquire the high energy necessary for the emission of curvature γ photons which are capable of producing electron-positron pairs. It is thus natural to look separately at the region of the double layer, which determines the conditions for the occurrence of "breakdown," and the region of quasineutral plasma, in which there is an effective multiplication of particles.

The scale of the double layer—its thickness H— can be estimated easily from Poisson equation (4.3). Examining the direction along the normal to the layer, h, and noting that the plasma density in the layer is low, we find

$$H \approx \left(\frac{|\Psi_c|\, c}{\Omega B \cos\chi}\right)^{1/2}. \tag{4.13}$$

Under the conditions prevailing in the magnetosphere of a pulsar we would have $H \sim 100$ m (with $\Psi_c \sim 10^{13}$ V). Since this quantity is not large, we can simplify the equations substantially. In the first place, the production of synchrotron photons will be inconsequential in comparison with curvature photons over distances comparable to H, and the scattering and loss of γ photons in pair production will also be inconsequential. We can therefore ignore the terms q_S, D, and $D_\perp$ in Eqs. (4.1) and (4.2). Furthermore, it can be shown that the effective production of electron-positron pairs by curvature γ photons occurs over a length scale Δh which is small in comparison with the thickness of the double layer. This result means that the plasma multiplication is a linear process: Each accelerated positron (for definiteness we are assuming that it is the positrons which are accelerated away from the star by the field) corresponds to K_H electrons which are produced near the upper boundary of the layer, $h = H$, and reflected back by the electric field:

$$n_e^-(H) = K_H n_e^+(0), \tag{4.14}$$

where $n_e^\pm(h)$ is the density of positrons or electrons. Analogously, near the surface of the star, $h = 0$, an electron accelerated by the field produces $K_\perp$ positrons. We can then write

$$n_e^+(0) = K_0 n_e^-(H), \qquad K_0 = K_\perp + K^+ + K_G. \tag{4.15}$$

Here we have used boundary condition (4.10), and we have assumed that there is no independent emission of positrons from the surface of the star: $F_{10}^+ = 0$. From (4.14) and (4.15) we find the following condition for a steady-state production of plasma, i.e., a "breakdown" condition:

$$K_0 K_H = 1. \tag{4.16}$$

The potential distribution in the layer is simple according to (4.3) and (4.12):

$$\Psi(h) = \Psi_c \frac{(H-h)^2}{H^2}, \qquad h \leqslant H. \tag{4.17}$$

At the upper boundary of the double layer, at $h = H$, the electric field vanishes; here the region of quasineutral plasma begins. To calculate the coefficients K_H and $K_\perp$ in (4.14) and (4.15) we need to solve the kinetic equations in the field (4.17). The corresponding calculation makes it possible to determine the critical potential Ψ_c, at which the condition for steady-state production, (4.16), holds and also the corresponding layer height H (Ref. 42). They can be written in the form[4)]

$$\Psi_c = 5.5\cdot 10^{12} \rho_7^{4/7} P^{-1/7} B_{12}^{-1/7} \cos^{1/7}\chi (1 - p i_0)^{1/7} b^{-2/7} \text{ V}$$
$$H = 9.5\cdot 10^3 \rho_7^{2/7} P^{3/7} B_{12}^{-4/7} \cos^{-3/7}\chi (1 - p i_0)^{-3/7} b^{-1/7} \text{ cm}; \tag{4.18}$$

here ρ is expressed in units of 10^7 cm, B in units of 10^{12} G, and P in seconds. We see that the critical potential is of the order of 10^{13} V and that the height is $H \sim 10^2$ m; neither depends strongly on the parameters of the pulsar. The parameter $p = (K-1)/(K+1)$, where $K = K^\pm + K_G$ is the total coefficient in (4.10), is a quantitative characteristic of the physical processes occurring at the surface. Specifically, this parameter shows how many secondary particles and γ photons with energies above 1 MeV are emitted from the surface when a single high-energy particle ($\varepsilon \sim 10^7$ MeV) is incident on it. The dimensionless parameter b also depends on the coefficient K, as shown in Fig. 10. With increasing K, the parameter b increases, so that the breakdown potential Ψ_c decreases. This decrease in Ψ_c, however, is quite slow: As K increases from 1 to 10^3, the potential Ψ_c falls off by a factor of about three. We can thus say that in the absence of independent emission the steady-state plasma production is not highly sensitive to the conditions at the surface of the pulsar.

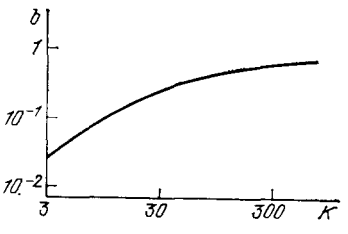

FIG. 10. The dimensionless parameter b as a function of the multiplication coefficient K.

Analogous plasma-production processes arise near a rotating neutron star when there is a free emission of charges of one sign (Arons *et al.*[56–58]).

The electric potential in the layer is described by (4.17) only if the layer height H is smaller than the radius of the polar cap, R_0, given by (2.4). As H approaches R_0, the breakdown potential Ψ_c tends toward its limiting value $\Psi_M = (B_0\Omega^2R^3/2c^2)\cos\chi$, given by (2.5). This limiting value may be lower than the value [given in (4.18)] required for plasma production in the layer. The result is a restriction on the parameters of the rotating neutron star,

$$PB_{12}^{-8/15} < 1.25b^{2/15}(K)\cos^{2/5}\chi, \tag{4.19}$$

under which an electron-positron plasma can be produced in the polar region of the star, i.e., under which the rotating neutron star can become a pulsar.

4.3. Plasma multiplication. In the region of quasineutral plasma, at $h > H$, there is an intense multiplication of electrons, positrons, and γ quanta. The source of the multiplication is a beam of fast positrons (or electrons) which is accelerated in the double layer to energies $\gamma \sim 10^7$–10^8. These primary particles, moving along the lines of force of the curvilinear magnetic field, emit curvature γ photons, which produce plasma. Equations (4.1)–(4.3) simplify in this case, since the electric field is essentially zero in a quasineutral plasma, so that the evolution of the distribution function is determined exclusively by the sequential cascade production of electron-positron plasma and radiation.

The evolution of the distribution function of the primary beam, $F_0(\gamma,h)$, is described by Eqs. (4.1) and (4.4):

$$\frac{\partial F_0}{\partial h} = \frac{2}{3}\alpha_f\frac{\lambda}{\rho^2}\frac{\partial}{\partial\gamma}\left[\gamma^4F_0 + \frac{55}{32\sqrt{3}}\frac{\lambda}{\rho}\frac{\partial}{\partial\gamma}(\gamma^7F_0)\right]. \tag{4.20}$$

At the boundary of the region of quasineutral plasma, $h = H$, the function F_0 is essentially monoenergetic:

$$F_0 = i_0\frac{K}{K+1}n_c\delta(\gamma-\gamma_0), \quad \gamma_0 = \frac{e|\Psi_c|}{mc^2}.$$

Solution of Eq. (4.20) shows that in the region of quasineutral plasma, $h > H$, the function F_0 becomes approximately Gaussian with a mean energy $\langle\gamma(h)\rangle$ and an energy spread $\Delta\gamma(h)$ (Ref. 42):

$$\langle\gamma\rangle = \gamma_0(1+3\eta)^{-1/3}, \quad \eta = \frac{2}{3}\alpha_f\lambda\gamma_0^3\int_H^h\frac{dh'}{\rho^2(h')}. \tag{4.21}$$

Here $\rho(h)$ is the radius of curvature of the magnetic field, given by (4.5). The energy spread $\Delta\gamma$ is small, $\sim 10^{-2}\gamma_0$, so that the slowing down of the primary beam is the primary process. The parameter η cannot exceed the maximum value

$$\eta_M = \frac{2}{3}\alpha_f\frac{\lambda R}{\rho_0^2}\gamma_0^3\ln\frac{c}{\Omega R}, \quad \rho_0 = \rho(h=0). \tag{4.22}$$

The total energy density lost by the primary beam is therefore

$$E_{max} = i_0n_c\frac{K}{K+1}\gamma_0mc^2[1-(1+3\eta_M)^{-1/3}]. \tag{4.23}$$

This energy is expended on the production of γ quanta and secondary plasma. We see that this energy is significant only if $\eta_M \gtrsim 1/3$; if $\eta_M < 1$, the energy expended on plasma production falls off sharply. The condition $\eta_M > 1/3$ leads to a limitation on γ_0, i.e., on the potential Ψ_c:

$$\Psi_c \gtrsim \Psi_k = 10^{13}P^{1/3}\left(\frac{f}{f^*}\right)^{-1/3}\ \text{V}; \tag{4.24}$$

here again, P is expressed in seconds. Only under the condition $\Psi_c\Psi_k$ is a significant amount of energy—of the order of the energy of the primary beam—expended on plasma production.

The secondary plasma is produced in stages. After the curvature γ photons from the primary beam have traversed a distance of the order of the mean free path $l(\varkappa)$,

$$l = \frac{4}{3}\frac{\rho}{\varkappa B_h\Lambda(\varkappa)}, \quad \Lambda(\varkappa) = \frac{1}{2}\ln\frac{\alpha_f\rho}{2\sqrt{6}\lambda B_h\varkappa^2}, \tag{4.25}$$

the curvature γ photons are absorbed, forming electron-positron pairs, which constitute the first generation of the plasma which is produced. In this case the energy of the particles lies in the interval

$$\frac{9}{8}\frac{\lambda}{\rho}\gamma_0^3B_h < \gamma < \frac{9}{8}\frac{\lambda}{\rho}\gamma_0^3B_h\Lambda\left(\frac{3}{2}\frac{\lambda}{\rho}\gamma_0^3\right),$$

and the spectrum of the particles is a power law, $\gamma^{-2/3}$. The next generation of plasma particles is produced by the synchrotron γ photons which are emitted during the formation of the first generation. Their energy lies in the interval

$$\frac{9}{8}\frac{\lambda}{\rho}\gamma_0^3B_h\Lambda^{-1}\left(\frac{3}{2}\frac{\lambda}{\rho}\gamma_0^3\Lambda^{-1}\right) < \gamma < \frac{9}{8}\frac{\lambda}{\rho}\gamma_0^3B_h,$$

and their spectrum is considerably steeper: $\gamma^{5/2}$ (etc.). At small values of γ, the cutoff of the spectrum of the plasma which is produced is determined by the transparency of the magnetosphere, since both the magnetic field B and the radius of curvature ρ vary substantially with height above the surface of the star. An analysis reveals

$$\gamma_{min} \approx 4\frac{\rho}{R} \approx 300-500, \tag{4.26}$$

where R is the radius of the star.

The plasma production usually terminates in the second generation, sometimes in the third. The energy spectrum of the particles of the plasma which is produced is shown in Fig. 11 (Ref. 44). We see that the particle distribu-

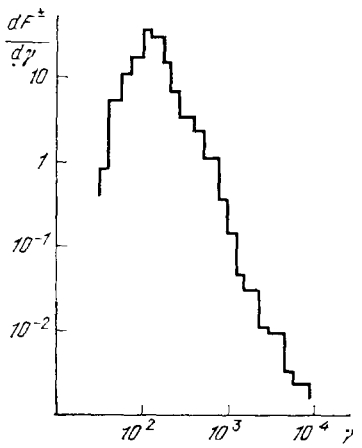

FIG. 11. Representative spectrum of a secondary electron-positron plasma produced by a primary particle with an energy of 10^{13} eV (Ref. 44).

tion function increases with decreasing energy of the particles at $\gamma > \gamma_{\min}$, in proportion to γ^{-2} on the average; at $\gamma < \gamma_{\min}$, the distribution function is cut off sharply.

5. RADIO EMISSION FROM A PULSAR

It was shown above that the plasma in the magnetosphere of a pulsar near open lines of force, $f < f^*$, is a steady stream of relativistic electrons and positrons with a Lorentz factor $\gamma \sim (3\text{–}5)\cdot 10^2$, which are moving along a very strong curvilinear magnetic field. Each individual charged particle emits electromagnetic waves. This is curvature radiation, completely analogous to ordinary synchrotron radiation having the same characteristic frequency $\omega_c = (3/2)(c/\rho)\gamma^3$ and being directed in a narrow cone with a vertex angle $\Delta\theta \sim 1/\gamma$ around the direction in which the particle is moving, i.e., along the magnetic field. This radiation was discussed in detail in the preceding section. In all cases, however, the discussion dealt with high-energy γ quanta, with a wavelength short in comparison with the average distance between particles. In this section of the review, we are concerned instead with the radiation which is generated by the main plasma and whose frequency is in the radio range, with a comparatively large wavelength $\lambda_r \sim 0.1\text{–}10^3$ cm. A study of this radiation under the conditions prevailing in a dense, relativistic plasma, in which the average distance between particles is much smaller than the wavelength of the radiated wave, so that collective effects are important, is of fundamental interest for reaching an understanding of the origin of the extremely intense and highly directional radio emission from pulsars.[64–68]

We wish to stress that in the steady state there is no radiation from the entire plasma, in contrast with the emission from an individual particle, since a constant current does not radiate. The curvilinear nature of the magnetic field, i.e., its nonuniformity, plays a governing role in the generation of this radiation. Yet another important circumstance is that since the velocity of all the plasma particles is close to the velocity of light, c, a Cherenkov interaction of the radiation with the plasma becomes possible for the normal oscillation mode with a refractive index slightly greater than unity. All or nearly all of the plasma particles are resonant particles in this case. The simultaneous coexistence and the interaction of the curvature and Cherenkov radiations should give rise to new oscillation modes, completely distinct from the oscillations of a homogeneous plasma.[45] We call these new modes "curvature-plasma modes."

5.1. Electrodynamics of an inhomogeneous plasma. To study the electrodynamic properties of such a medium as an inhomogeneous, collisionless, relativistic electron-positron plasma, it is first necessary to calculate the dielectric permittivity tensor. To do this, we first use a path-integration method to solve the linearized kinetic equation and to find the response of the inhomogeneous medium to a plane wave with a wave vector $\mathbf{k}$ and a frequency ω. The general expression for the current $\mathbf{j}$ induced in the medium by the plane wave is written[69]

$$\mathbf{j}(\omega,\ \mathbf{k},\ \mathbf{r},\ t)$$

$$= -e^2 \int \mathrm{d}\mathbf{p}\mathbf{v} \int_{-\infty}^{t} \exp(-i\omega t' + i\mathbf{k}\mathbf{r}')$$

$$\times\left(\mathbf{E}_A + \left[\frac{\mathbf{v}'}{\omega}[\mathbf{k}\mathbf{E}_A]\right]\right)\frac{\partial F}{\partial \mathbf{p}'}\,\mathrm{d}t'; \qquad (5.1)$$

here $\mathbf{E}_A$ is the amplitude of the electric field of the wave; $F(\mathbf{p},\mathbf{r})$ is the unperturbed distribution function of the particles of charge e; and $\mathbf{p}' = \mathbf{p}(t')$, $\mathbf{v}' = \mathbf{v}(t')$, and $\mathbf{r}' = \mathbf{r}(t')$ are the momentum, velocity, and coordinate at the time t' of a particle moving along an unperturbed path, so that at the time t the particle is at the point under consideration, $\mathbf{r}$, and has a momentum $\mathbf{p}$ and a velocity $\mathbf{v}$. Using this expression for the current, and assuming $j_\alpha = \sigma^0_{\alpha\beta}E_\beta \times \exp(-i\omega t + i\mathbf{k}\mathbf{r})$, where $\sigma^0_{\alpha\beta}$ is the conductivity of the medium, we find the corresponding dielectric permittivity in the standard way:

$$\varepsilon^{(0)}_{\alpha\beta} = \delta_{\alpha\beta} + \frac{4\pi i}{\omega}\sigma^0_{\alpha\beta},$$

$$\varepsilon^0_{\alpha\beta}(\omega,\ \mathbf{k},\ \mathbf{r}) = \delta_{\alpha\beta} - \frac{4\pi i e^2}{\omega}$$

$$\times \int \mathrm{d}\mathbf{p} v_\alpha \int_{-\infty}^{t} \mathrm{d}t' \exp[i\omega(t-t') - i\mathbf{k}(\mathbf{r}-\mathbf{r}')]$$

$$\times\left[\left(1 - \frac{\mathbf{k}\mathbf{v}'}{\omega}\right)\delta_{\beta\sigma} + \frac{k_\sigma v'_\beta}{\omega}\right]\frac{\partial F}{\partial p'_\sigma}. \qquad (5.2)$$

It should be kept in mind, however, that the quantity $\varepsilon^0_{\alpha\beta}(\omega,\mathbf{k},\mathbf{r})$ in (5.2) is not the quantity which determines the dispersion properties of the inhomogeneous medium and which must be substituted into the dispersion relation in order to find the natural modes and eigenfrequencies of electromagnetic oscillations. The point is that although we have taken into account the effect of the inhomogeneity of the medium on the motion of the particles the electromagnetic wave was assumed to be a plane wave, as in a homogeneous medium. Plane waves, however, are not eigenfunctions in an inhomogeneous plasma.

In the case of a slightly inhomogeneous medium, in which the wavelength is much shorter than the scale of the inhomogeneity (in our case, this scale is the radius of curvature of the magnetic field, ρ),

$$k\rho \gg 1 \qquad (5.3)$$

and the damping (or growth) of the wave is relatively slight,

$$\frac{|\mathrm{Im}\,\mathbf{k}|}{|\mathbf{k}|} \sim \frac{|\varepsilon^{\mathrm{aH}}|}{|\varepsilon^{\mathrm{H}}|} \ll 1, \quad \varepsilon_{\alpha\beta} = \varepsilon^{\mathrm{H}}_{\alpha\beta} + i\varepsilon^{\mathrm{aH}}_{\alpha\beta} \qquad (5.4)$$

($\varepsilon^{\mathrm{H}}_{\alpha\beta}$ is the Hermitian part, and $\varepsilon^{\mathrm{aH}}_{\alpha\beta}$ the anti-Hermitian part, of the tensor $\varepsilon_{\alpha\beta}$), we can choose the field of a wave packet as eigenfunctions for the electromagnetic field:

$$\mathbf{E}(\mathbf{r}) = \mathbf{E}^0(\mathbf{r})\exp[i\Phi(\mathbf{r})].$$

Using the energy transport equation, we can show that the equation for the electromagnetic field of the wave then takes the usual form

$$\left(k_\alpha k_\beta - k^2\delta_{\alpha\beta} + \frac{\omega^2}{c^2}\varepsilon_{\alpha\beta}\right) E_\beta^0 = 0, \tag{5.5}$$

if the quantity $\varepsilon_{\alpha\beta}(\omega,\mathbf{k},\mathbf{r})$ in (5.5) is related to the quantity $\varepsilon^0_{\alpha\beta}(\omega,\mathbf{k},\mathbf{r})$ by

$$\varepsilon_{\alpha\beta}(\omega,\ \mathbf{k},\ \mathbf{r}) = \frac{1}{(2\pi)^3}\int d\mathbf{k}'\, d\mathbf{R}'\varepsilon^0_{\alpha\beta}\left(\omega,\ \mathbf{k}',\ \mathbf{r}+\frac{\mathbf{R}'}{2}\right)$$

$$\times\exp\left[i(\mathbf{k}'-\mathbf{k})\mathbf{R}'\right]. \tag{5.6}$$

It follows from (5.5) that the quantity $\varepsilon_{\alpha\beta}(\omega,\mathbf{k},\mathbf{r})$ is the dielectric permittivity tensor of a slightly inhomogeneous medium which we have been seeking.

Expression (5.2), (5.6) for $\varepsilon_{\alpha\beta}$ can be simplified. For this purpose, we substitute (5.2) into (5.6) and integrate over $d\mathbf{k}'$ and $d\mathbf{R}'$. Since the quantity $\mathbf{r}-\mathbf{r}'$ in (5.2) is a function of the coordinate $\mathbf{r}$, the momentum $\mathbf{p}$, and the time difference $t-t'$,

$$\mathbf{r}-\mathbf{r}' = \mathbf{L}(\mathbf{r},\ \mathbf{p},\ t-t'),$$

we find[45]

$$\varepsilon_{\alpha\beta} = \delta_{\alpha\beta} - \frac{4\pi ie^2}{\omega}\int d\mathbf{p} v_\alpha \int_{-\infty}^{t} dt' \exp\left[i\omega(t-t') - i\mathbf{k}\mathbf{R}^*\right]$$

$$\times \det{}^{-1}\left|\delta_{\mu\nu} - \frac{\partial L_\mu\left(\mathbf{r}+\frac{\mathbf{R}^*}{2}\right)}{2\partial r_\nu}\right|\left[\left(1-\frac{\mathbf{k}\mathbf{v}'}{\omega}\right)\delta_{\beta\sigma}\right.$$

$$\left. + \frac{k_\sigma v'_\beta}{\omega} + \frac{i}{2\omega}\frac{\partial}{\partial r_\sigma}\cdot v'_\beta - \frac{i}{2\omega}\delta_{\beta\sigma}\frac{\partial}{\partial r_\chi}\cdot v'_\chi\right]\frac{\partial F}{\partial p'_\sigma}\Big|_{\mathbf{r}=\mathbf{r}+(\mathbf{R}^*/2)}, \tag{5.7}$$

where the vector $\mathbf{R}^*(\mathbf{r},\mathbf{p},t-t')$ is the solution of the equation

$$\mathbf{R}^* = \mathbf{L}\left(\mathbf{r}+\frac{\mathbf{R}^*}{2},\ \mathbf{p},\ t-t'\right). \tag{5.8}$$

5.2. Dielectric permittivity. Expression (5.7) holds for any inhomogeneous medium under conditions (5.3) and (5.4). Let us calculate the quantity $\varepsilon_{\alpha\beta}(\omega,\mathbf{k},\mathbf{r})$ for our case, in which the medium is an electron-positron plasma moving at a relativistic velocity along a curved magnetic field. At each given point $\mathbf{r}$ we introduce three unit vectors: $\mathbf{b}$, along the direction of the magnetic field; $\mathbf{n}$, the normal vector; and $\mathbf{l}$, the binormal vector. Since the particles are moving along the magnetic field, their distribution function is of the form in (3.3):

$$F(\mathbf{p},\ \mathbf{r}) = n_e F_\parallel(p_\parallel)\,\delta(\mathbf{p}_\perp); \tag{5.9}$$

here $p_\parallel$ is the momentum component along $\mathbf{b}$, and $\mathbf{p}_\perp$ is that transverse to $\mathbf{b}$. Here we have taken into account the circumstance that the transverse drift of the particles is slight ($|\mathbf{p}_\perp| < p_\parallel$) in the part of the magnetosphere in which we are interested. By virtue of the relation $\omega \ll \omega_B$ (ω_B is the cyclotron frequency), a possible transverse motion of the particles "is rapidly forgotten," and we can write

$$\frac{\partial F}{\partial p'_\sigma} = n_e b_\sigma(\mathbf{r}')\frac{\partial F_\parallel}{\partial p_\parallel}\delta(\mathbf{p}_\perp) = n_e\frac{v_\sigma(t')}{v_\parallel}\frac{\partial F_\parallel}{\partial p_\parallel}\delta(\mathbf{p}_\perp).$$

To pursue the calculations we need to know the paths along which the particles move:

$$\mathbf{r} = \mathbf{r}' + \mathbf{v}(t-t') - \frac{\mathbf{a}}{2}(t-t')^2 + \frac{\dot{\mathbf{a}}}{6}(t-t')^3 + \ldots,$$

$$\mathbf{a} = \frac{v_\parallel^2}{\rho}\mathbf{n};\quad \dot{\mathbf{a}} = -\frac{v_\parallel^3}{\rho^2}\mathbf{b} - \frac{v_\parallel^3}{\rho^2}\mathbf{n}\left(\mathbf{b}\frac{\partial\rho}{\partial\mathbf{r}}\right) - \frac{v_\parallel^3}{\rho\rho_\tau}\mathbf{l}; \tag{5.10}$$

here ρ is the radius of curvature in (4.5), and ρ_τ is the radius of the twisting of a magnetic line of force. Since the relation $\rho_\tau \gg \rho$ holds in the region in which the radiation is excited, we will set $\rho_\tau = \infty$ for the discussion below. The value of the distribution function at the point $\mathbf{r} + (R^*/2)$ appears in expression (5.7) for the dielectric permittivity tensor. We thus also need to find the particle velocities $\mathbf{v}$ and $\mathbf{v}(t')$ and $\mathbf{R}^*$ at the point $\mathbf{r} + (\mathbf{R}^*/2)$. We have

$$\mathbf{w} = v_\parallel\mathbf{b}\left(\mathbf{r}+\frac{\mathbf{R}^*}{2}\right)$$

$$= v_\parallel\mathbf{b} + \frac{v_\parallel^2}{2\rho}(t-t')\mathbf{n} - \frac{1}{8}\frac{v_\parallel^3}{\rho^2}(t-t')^2\left[\mathbf{b}+\mathbf{n}\left(\mathbf{b}\frac{\partial\rho}{\partial\mathbf{r}}\right)\right],$$

$$\mathbf{v}'(\mathbf{w}) = v_\parallel\mathbf{b} - \frac{v_\parallel^2}{2\rho}(t-t')$$

$$\times\mathbf{n} - \frac{1}{8}\frac{v_\parallel^3}{\rho^2}(t-t')^2\left[\mathbf{b}+\mathbf{n}\left(\mathbf{b}\frac{\partial\rho}{\partial\mathbf{r}}\right)\right], \tag{5.11}$$

$$\mathbf{R}^*(\mathbf{w}) = v_\parallel\mathbf{b}(t-t') - \frac{1}{24}\frac{v_\parallel^3}{\rho^2}(t-t')^3\left[\mathbf{b}+\mathbf{n}\left(\mathbf{b}\frac{\partial\rho}{\partial\mathbf{r}}\right)\right].$$

It is important to note that $\mathbf{R}^*$ in (5.11) is an odd function of the difference $(t-t')$. In general, it can be shown that the quantity $\omega(t-t') - \mathbf{k}\mathbf{R}^*$ in (5.7) is an odd function of the argument $t-t'$. This situation corresponds to the fact that time reversal ($t \to -t$) leaves the dielectric permittivity tensor $\varepsilon_{\alpha\beta}$ the same for the inverted wave ($\omega = -\omega$, $\mathbf{k} = -\mathbf{k}$). This important property determines the possibility of a local description of the inhomogeneous medium. The tensor $\varepsilon^0_{\alpha\beta}$ in (5.2) does not have this property.

Substituting expressions (5.11) into (5.7), we find the following expression for the dielectric permittivity tensor which we are seeking:

$$\varepsilon_{\alpha\beta}(\omega,\ \mathbf{k},\ \mathbf{r})$$

$$= \delta_{\alpha\beta} - \frac{i\omega_p^2}{\omega}\int dp_\parallel m v_\parallel\frac{\partial F_\parallel}{\partial p_\parallel}\int_0^\infty d\tau E_{\mathbf{x}p}(\omega,\ \mathbf{k},\ p_\parallel,\ \tau)$$

$$\times\left[b_\alpha b_\beta\left(1-\frac{v_\parallel^2\tau^2}{4\rho^2}\right)\right.$$

$$+ (n_\alpha b_\beta - n_\beta b_\alpha)\frac{v_\parallel}{2\rho}\tau$$

$$\left. - (n_\alpha b_\beta + n_\beta b_\alpha)\tau^2\left(\mathbf{b}\frac{\partial\rho}{\partial\mathbf{r}}\right)\frac{v_\parallel^2}{8\rho^2} - n_\alpha n_\beta\frac{v_\parallel^2}{4\rho^2}\tau^2\right], \tag{5.12}$$

$$E_{\mathbf{x}p}(\omega,\ \mathbf{k},\ p_\parallel,\ \tau)$$

$$= \exp\left\{i\left[\omega - (\mathbf{k}\mathbf{b})v_\parallel\right]\tau + \frac{i}{24}\frac{v_\parallel^3}{\rho^2}\tau^3\left[(\mathbf{k}\mathbf{b}) + (\mathbf{k}\mathbf{n})\left(\mathbf{b}\frac{\partial\rho}{\partial\mathbf{r}}\right)\right]\right\};$$

here $\omega_p^2 = 4\pi e^2 n_e/m$ is the plasma frequency. Considering modes which are propagating at a small angle $\theta \sim 1/\gamma$ from the magnetic field (since only such modes could be unstable), we can ignore the terms containing the derivative of the radius of curvature, $\partial\rho/\partial\mathbf{r}$. Integrating over τ in (5.12), we can write the tensor $\varepsilon_{\alpha\beta}$ in the following final form[45]:

$$\varepsilon_{\alpha\beta}=\begin{Vmatrix} 1+4\pi\omega_p^2\frac{\rho^{2/3}}{k_z^{4/3}}\left\langle\frac{\mathrm{Gi}'''(\xi)-i\mathrm{Ai}'''(\xi)}{\gamma^3 v_\parallel^2}\right\rangle, & 0, & -4\pi\omega_p^2\frac{\rho}{k_z}\left\langle\frac{\mathrm{Ai}''(\xi)+i\mathrm{Gi}''(\xi)}{\gamma^3 v_\parallel^2}\right\rangle \\ 0, & 1, & 0 \\ 4\pi\omega_p^2\frac{\rho}{k_z}\left\langle\frac{\mathrm{Ai}''(\xi)+i\mathrm{Gi}''(\xi)}{\gamma^3 v_\parallel^2}\right\rangle, & 0, & 1+4\pi\omega_p^2\frac{\rho^{4/3}}{k_z^{2/3}}\left\langle\frac{\mathrm{Gi}'(\xi)-i\mathrm{Ai}'(\xi)}{\gamma^3 v_\parallel^2}\right\rangle \end{Vmatrix}. \tag{5.13}$$

The Airy functions $\mathrm{Ai}(\xi)$ and $\mathrm{Gi}(\xi)$ are defined by

$$\mathrm{Ai}(\xi)+i\mathrm{Gi}(\xi)=\frac{1}{\pi}\int_0^\infty \exp\left(i\xi t+\frac{it^3}{3}\right)dt;$$

the primes in (5.13) mean the derivatives with respect to the argument

$$\xi=2(\omega-k_z v_\parallel)\frac{\rho^{2/3}}{k_z^{1/3}v_\parallel}. \tag{5.14}$$

The coordinate system has been chosen in such a way that the z axis runs along the vector **b**, while x runs along **n**. The angle brackets mean an average over the distribution function $F_\parallel(p_\parallel)$: $\langle\ldots\rangle=\int dp_\parallel\ldots F_\parallel(p_\parallel)$.

In the limit $\rho\to\infty$, expression (5.13) becomes the corresponding expression for an inhomogeneous plasma with[45] $\omega\ll\omega_B=eB/mc\gamma$:

$$\varepsilon_{xx}=\varepsilon_{yy}=1,$$
$$\varepsilon_{zz}=1-\left\langle\frac{\omega_p^2}{\gamma^3(\omega-k_z v_\parallel)^2}\right\rangle,$$
$$\varepsilon_{xy}=\varepsilon_{yx}=\varepsilon_{xz}=\varepsilon_{zx}=\varepsilon_{yz}=\varepsilon_{zy}=0.$$

For finite values of ρ and for $\omega\approx k_z v_\parallel\approx k_z c$, however, the dielectric permittivity of the inhomogeneous plasma in (5.13) has essentially nothing in common with the local dielectric permittivity of a homogeneous medium. This result is not surprising: In the first place, there is no curvature radiation in a homogeneous medium, since curvature radiation is due entirely to an inhomogeneity. Furthermore, the entire plasma consists of resonant particles, and under the condition $\xi\lesssim 1$ (and also at all negative values of ξ) the imaginary part of the increment in the unit tensor $\delta_{\alpha\beta}$ is comparable in order of magnitude to the real part. This circumstance gives rise to new oscillation modes with a significant growth rate which do not exist in a homogeneous plasma.

5.3. Curvature-plasma modes. We turn now to normal waves. We begin by noting that a wave polarized in such a way that its electric vector is directed perpendicular to the (x,z) plane does not interact with the plasma. It is simple to see that this would be an ordinary vacuum wave with a refractive index $n\equiv 1$. The properties of the other normal modes, which are polarized in the plane of motion of the particles, depend strongly on the parameter a:

$$a=4\pi\left\langle\frac{1}{\gamma^3}\right\rangle\omega_p^2\frac{\rho^{4/3}}{k_z^{2/3}c^2}. \tag{5.15}$$

If $a\gg 1$, $(\omega/\omega_c)^{2/3}\gg a$ (region II; see Fig. 12), then two longitudinal waves and one transverse wave in the radio-frequency range can propagate in the magnetospheric plasma, as in the case of a uniform magnetic field. Under the condition $a\gg 1$, $(\omega/\omega_c)^{2/3}\ll a$ (region I) in contrast, one of the plasma waves splits in three. Two of the three turn out to be unstable at angles $\theta<\theta_{1,2}$ where θ is the angle between **k** and **B**:

$$\theta_{1,2}=u_{1,2}\frac{a}{(k_z\rho)^{1/3}},\quad u_1=0{,}15,\quad u_2=0.41. \tag{5.16}$$

This splitting of modes is illustrated in Fig. 13 for the case $\omega_p^2\langle\gamma\rangle/\omega^2\gg 1$. The imaginary parts of the refractive index,

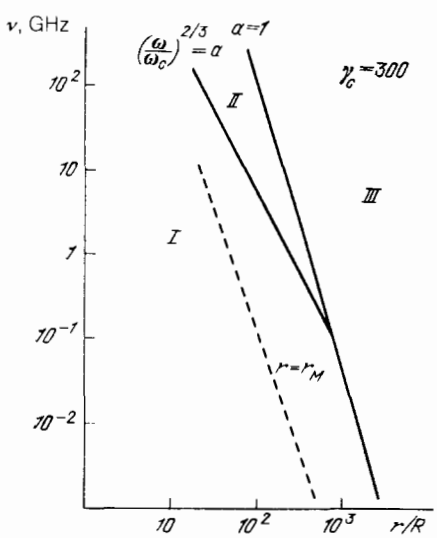

FIG. 12. Three regions of parameter values which are distinguished in the magnetosphere of a pulsar. Maser amplification of curvature-plasma modes occurs in region I. Only two transverse waves can propagate in region III. The dashed line corresponds to the height r_M in (5.21); this is the height at which unstable waves leave the amplification cone.

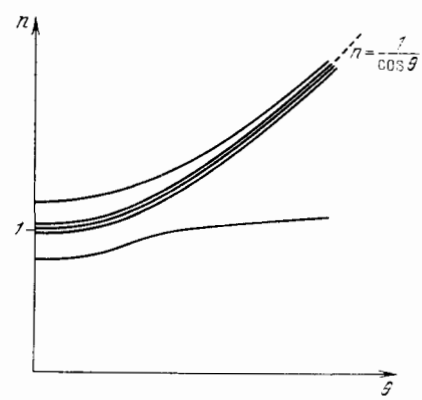

FIG. 13. Dispersion curves for the five normal waves which exist in region I. The unstable curvature-plasma modes correspond to drift oscillations with $n\approx 1/\cos\theta$.

which give us the growth rates of the unstable curvature-plasma modes, can be written as follows[45] for sufficiently small angles θ:

$$\operatorname{Im} n \approx \left\langle \frac{1}{\gamma^3} \right\rangle^{1/5} \frac{\omega_p^{2/5}}{k_z^{4/5} c^{2/5} \rho^{2/5}}. \qquad (5.17)$$

It can be seen from Fig. 13 that unstable curvature-plasma waves correspond to drift oscillations for which we would have $n \approx 1/\cos\theta$.

In region III, where the condition $a \ll 1$ holds, only a single transverse wave with $n \approx 1$, can propagate. The damping and excitation of this wave are of minor importance and can in fact be ignored.

We wish to stress that the growing solutions in (5.17) correspond to a hydrodynamic instability. This is as it should be, since the limit $a \gg 1$ corresponds to a high particle density, as can be seen from (5.14). Further indication that the instability is of a hydrodynamic nature comes from the circumstance that the imaginary parts in (5.17) depend on the particle density in a power-law fashion: $\operatorname{Im} n \propto n_e^{1/5}$ (we are using $\omega_p^2 \propto n_e$).

Now using (2.2) and (4.5), we conclude that in the case of a dipole magnetic field $B \approx B_0 (r/R)^{-3}$ the parameter a depends only on the line of force f, the wave frequency ν, and the distance (r) from the center of the star:

$$a = 5{,}5 \cdot 10^6 \nu_{\mathrm{GHz}}^{2/3} P^{-1/3} \gamma_{300}^{-3} B_{12} \lambda_3 \left(\frac{r}{R}\right)^{-7/3} \left(\frac{f}{f^*}\right)^{2/3} \qquad (5.18)$$

[ν is expressed in gigahertz; $\langle 1/\gamma^3 \rangle^{-1/3}$ is expressed in units of $\gamma_0 = 300$; we are using $\lambda_3 = \lambda/10^3$ as in (3.9); and B is expressed in units of 10^{12} G]. As a result (Fig. 12), region I, in which rapidly growing curvature-plasma waves propagate, is in the inner magnetosphere, i.e., close to the star, with $r/R \sim 10$–100, while region III, in which only two transverse waves propagate, is in the more remote outer magnetosphere. The frequency corresponding to the nodal point,

$$\nu^* = 60 \gamma_{300}^{17/4} B_{12}^{-1/4} \lambda_3^{-1/4} P^{-1/2} \left(\frac{f}{f^*}\right)^{3/4} \text{MHz}, \qquad (5.19)$$

falls in the center of the observable radio-frequency range for the typical parameter values ($\gamma_c \sim 400$–500, $B \sim 10^{12}$ G). We wish to emphasize that ν^* is a very strong function of the characteristic energy of the particles:

$$\gamma_c = \langle 1/\gamma^3 \rangle^{-1/3}.$$

What is the total optical thickness traversed by unstable curvature-plasma waves as they propagate in the inner magnetosphere? Using asymptotic expression (5.17), we find

$$\tau_{1,2} = 2\frac{\omega}{c} \int \operatorname{Im} n \, dl$$

$$= -290 s_{1,2} \nu_{\mathrm{GHz}}^{1/5} \gamma_{300}^{-3/5} P^{-2/5} \lambda_3^{1/5} B_{12}^{1/5} \left(\frac{f}{f^*}\right)^{1/5}, \qquad (5.20)$$

where $s_{1,2}$ is a geometric factor of order unity.

Figure 14 shows the total thickness τ_1 as a function of the frequency ν. The paths of normal waves were calculated in the geometrical optics approximation. Although the group velocity of the waves is directed along the magnetic line of force, the wave vector $\mathbf{k}$ deviates systematically from the direction of the magnetic field. As a result, at angles $\theta > \theta_{1,2}$ [see (5.16)] the waves no longer grow. That height above the surface of the star at which the waves leave the growth "cone" is determined by

$$r_M = 50 R \cdot \gamma_{300}^{-1} \nu_{\mathrm{GHz}}^{-1/3} B_{12}^{1/3} \lambda_3^{1/3} \left(\frac{f}{f^*}\right)^{-1/3}. \qquad (5.21)$$

The value $r = r_M$ is shown by the dashed line in Fig. 12.

We see from Fig. 14 that the modulus of the optical thickness is a few hundred. This value corresponds to an amplification by a factor of $e^{300} \sim 10^{100}$! This result of course does not mean that such a huge amplification actually occurs: Nonlinear processes will act to limit the radiation power long before this amplification is achieved.

In summary, a relativistic plasma moving along a strong curvilinear magnetic field is unstable. The instability, which leads to a growth of electromagnetic waves, is of a hydrodynamic nature. It is related to a Cherenkov excitation of curvature-plasma modes and has high growth rates. Under the conditions prevailing in the magnetosphere of a pulsar, this instability leads to an intense excitation of oscillations of the field and of the plasma in the region of broken lines of force. At a distance of (10–100)R from the neutron star, these oscillations convert into ordinary radio waves, with frequencies over the range 0.01–10 GHz. The radio waves emerge from near the magnetic poles of the star and are directional. The picture found here thus corresponds completely to the generally accepted model for the radio emission of a pulsar (Fig. 1).

6. COMPARISON OF THEORY AND OBSERVATIONAL DATA

6.1. Structure of the active region. Having determined the potential drop in the region in which the particles are accelerated and produced, we can now compare the theory with observational data. Using the potential drop in the acceleration region, given in (4.18), we can find the parameter β_0 which appears in compatibility relation (3.25), and we can thereby determine the longitudinal current circulating in the magnetosphere, i_0. The longitudinal current i_0 specifies the total energy loss of the neutron star, according to (3.37). This loss can be detemined from observations.

It is natural to suggest that the longitudinal current i_0 is constant over the entire plasma production region. Relation (4.18) for magnetic fields $B < 0.1 B_c$ then leads to the following dependence of the dimensionless ratio Ψ_c/Ψ_M on the

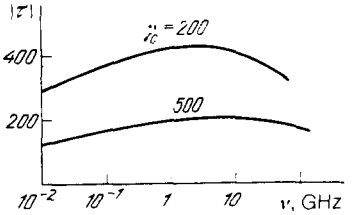

FIG. 14. Modulus of the optical thickness traversed by unstable curvature-plasma waves as a function of the frequency ν.

quantity $f = B_0 r_\perp^2/2$, which characterizes a given line of force at the surface of the star and which is proportional to the square of the distance ($r_\perp$) from the given line of force to the magnetic axis:

$$\frac{\Psi_c}{\Psi_M} = a_0 B_{12}^{-8/7} P^{15/7} \cos^{1/7}\chi\,(1 - pi_0)^{1/7}\left(\frac{f}{f^*}\right)^{-2/7}. \qquad (6.1)$$

Here $a_0 \approx 1$, and Ψ_M is the maximum possible potential drop in the acceleration region [expression (2.5)]. The region of magnetic lines of force f in which a steady-state solution can exist is determined by the two conditions

$$\Psi_c(f^*) = 0, \qquad (6.2)$$

$$-1 \leqslant \frac{c}{\Omega}\frac{d\Psi_c}{df} \leqslant 0, \qquad (6.3)$$

which follow from (3.16) and (3.22). If the first of these conditions does not hold, the current flowing from the surface of the pulsar cannot return to the star. If the second condition $(c/\Omega)d\Psi_c/df < -1$) does not hold, the plasma in the region of broken lines of force will rotate in the direction opposite to the rotation of the star. This of course can not be the case.

Figure 15 shows values of f satisfying conditions (6.2) and (6.3). Consequently, the plasma on the broken lines of force is produced continuously only in the annular region

$$f_1 < f < f_2, \qquad (6.4)$$

where

$$\frac{f_1}{f^*} = \left(\frac{2}{9}q_f\right)^{7/9}, \qquad \frac{f_2}{f^*} = 1 - q_f\left(\frac{f_2}{f^*}\right)^{-2/7}, \qquad (6.5)$$

and

$$q_f = a_f B_{12}^{-8/7} P^{15/7}\cos^{1/7}\chi\,(1 - pi_0)^{1/7}, \qquad a_f \approx 1. \qquad (6.6)$$

The pattern of currents flowing in the magnetosphere can thus be described as follows: At $f < f_1$, i.e., at $r_\perp < r_{in}$, where

$$\frac{r_{in}}{R_0} \simeq a_R P^{5/6} B_{12}^{-4/9}\cos^{-1/3}\chi; \qquad a_R \approx 1, \qquad (6.7)$$

and R_0 is the radius of the polar cap, given in (2.4), there are no currents, and no plasma is produced here. A hollow region thus forms inside the plasma-filled magnetosphere. This fact reflects a particular feature of the plasma production in our model (a "hollow cone").[54]

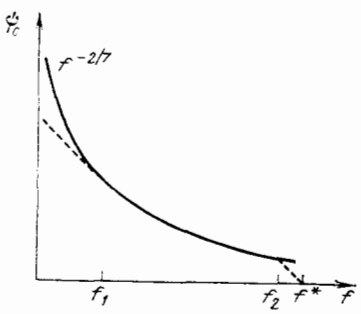

FIG. 15. Region of continuous plasma production, $f_1 < f < f_2$. The dashed line corresponds to a slope $(\Omega/c)d\Psi_c/df = -1$.

Further on, at the boundary $r_\perp = r_{in}$, as was shown in Ref. 41, there is a jet of surface current,

$$I_{in} = 2\frac{B_0\Omega^2 R^3}{c} - \frac{f_1/f^*}{i_0}, \qquad (6.8)$$

and then comes a region of constant production of an electron-positron plasma. The total current flowing in this region is determined by compatibility relation (3.25), where, according to (6.1), we have

$$\beta_0 = a_\beta B_{12}^{-8/7} P^{15/7}\cos^{1/7}\chi\,(1 - pi_0)^{1/7}, \qquad a_\beta \simeq 1. \qquad (6.9)$$

The density of the current which is flowing out is here generally lower than that of the current near the inner boundary of the hollow cone. Finally, the entire current returns to the star along the separatrix $f = f^*$ (i.e., $r_\perp = R_0$).

We wish to emphasize that the numerical proportionality coefficients a_0, a_f, a_R, and a_β are of order unity. Everywhere below we will set them equal to unity, since there seems to be no point in calculating them more accurately. In the first place, they depend on such quantities as the moment of inertia I_r and the radius R of the star; the radius R appears raised to the sixth power, as can be seen in, for example, (3.37). The theories which have been derived for the internal structure of neutron stars lead to an uncertainty of at least 100% in the coefficients, because of the uncertainty in I_r and R[6] (Ref. 3). Second, as we have already mentioned, relation (3.25) was derived under the assumption that the following condition holds in the plasma production region:

$$\beta_0 = \frac{\Omega}{c_{ii}}\frac{d\Psi}{df} = \text{const}.$$

As can be seen from Fig. 15, the accelerating potential in (4.18) and (6.1) does not satisfy this condition. The result is again to introduce a significant uncertainty.

To pursue the analysis we need to determine the basic characteristics of the pulsars in terms of the observable quantities P and dP/dt. It is convenient for this purpose to introduce the dimensionless parameter

$$Q = 2P^{11/10}\dot{P}_{-15}^{-4/10}, \qquad (6.10)$$

where $\dot{P}_{-15} = 10^{15} dP/dt$ is the rate at which the pulsar is slowing down. Now using Eq. (3.35) to determine the magnetic field B_0 in terms of the observable quantities P and dP/dt and the nonobservable quantity $\cos\chi$, and also using the asymptotic form of compatibility relation (3.25),

$$i_0 = i_M(\chi)\left(\frac{2\beta_0}{\beta_M(\chi)}\right)^{1/2}, \qquad (6.11)$$

which holds at $i_0 \ll i_M(\chi)$, $\beta_0 \ll \beta_M(\chi)$, we find

$$\frac{\beta_0}{\beta_M(\chi)} \approx Q^2, \qquad (6.12)$$

$$\frac{r_{in}}{R_0} \approx Q^{7/9}. \qquad (6.13)$$

The dependence on the angle χ in (6.12) and (6.13) is unimportant.[41] The magnetic field,

$$B_{12} \approx P^{-1/20}\dot{P}_{-15}^{7/10}\cos^{-1}\chi, \qquad Q < 1, \qquad (6.14)$$

on the other hand, depends strongly on χ.

We see that for pulsars with $Q < 1$ the inner radius of the

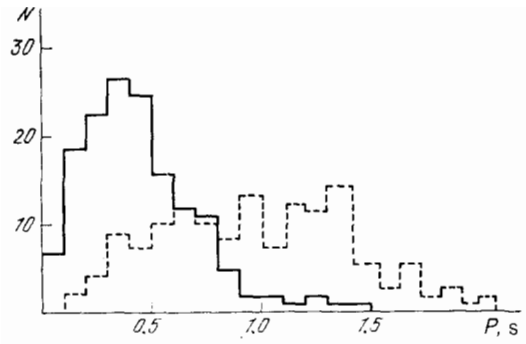

FIG. 16. Distributions in the period P for "young" pulsars ($Q < 1$; solid line) and "old" pulsars ($Q > 1$; dashed line).

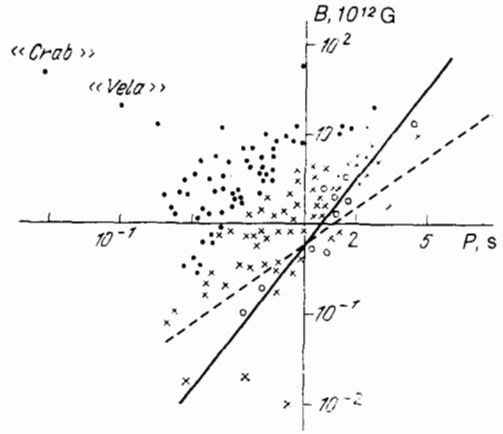

FIG. 17. Pulsar extinction boundary on a (P,B_{12}) diagram. The region to the left of the boundary is the region of steady-state plasma production. Filled points—pulsars with $Q < 1$; crosses—pulsars with $Q > 1$; open circles—extinguishing pulsars, i.e., those which have an irregular emission[42]; dashed line—the boundary $\eta_M = 1/3$, to the right of which the energy lost by the primary beam is small.

outflowing plasma, r_{in}, is smaller than R_0, and the relation $\beta_0 < \beta_M(\chi)$ holds. Consequently, the outflowing current covers essentially the entire surface of the polar cap for pulsars with $Q < 1$, so that for such pulsars we can indeed use compatibility relation (3.25) or, more precisely, its asymptotic form in (6.11). For pulsars with $Q > 1$ we set $r_{in} \approx R_0$ and $\beta_0 \approx \beta_M(\chi)$. This approach results in the following expression for the magnetic field of pulsars with $Q > 1$:

$$B_{12} \approx P^{15/8} \cos^{-1} \chi, \qquad Q > 1. \tag{6.15}$$

Figure 16 shows the period distribution of 300 pulsars for which the slowing rate dP/dt is presently known.[24,25] The solid line represents 152 pulsars with $Q < 1$, while the dashed line represents 148 with $Q > 1$. We see that most of the pulsars with $Q > 1$ have periods $p > 0.7$ s, while the periods of pulsars with $Q < 1$ are shorter than 0.8 s for the most part.

In the literature, the question of a significant difference between the properties of pulsars with long and short periods has been raised repeatedly on the basis of analyses of observational data.[70] We will now show that the observed difference in the properties of radiopulsars is related to the parameter Q and can be explained on the basis of the theory which has been derived.

6.2. Plasma production. In the first place, the quantity Q characterizes the rate at which the electron-positron plasma is produced near the magnetic poles of the neutron star. As can be seen from (6.13), the production of plasma in the case of pulsars with $Q > 1$ should be suppressed, for plasma production in such pulsars occurs only in a thin ring with $r_{in} \approx R_0$.

Figure 17 shows the distribution of pulsars in the plane defined by the period and the magnetic field, whose values were found from (6.14) and (6.15) with $\cos \chi = 0.5$. We see that all the pulsars whose radio emission reveals various irregularities (a "turning off," a "switching," and a drift of subpulses) do in fact lie in the region $Q > 1$. All the pulsars with $Q < 1$, on the other hand, are characterized by stable radio emission.[41]

Furthermore, as is easily verified, condition (4.19), which determines the possibility of steady-state plasma production (i.e., whether a radiopulsar can exist) can be written as $Q < Q_0$, where

$$Q_0 = 2.5 b^{1/7}. \tag{6.16}$$

From Fig. 17 we see that this condition corresponds well to observational data.[21]

It follows from a comparison of (6.16) with the observed boundary of the distribution of pulsars, shown in Fig. 17, that we have $b(K) \approx 0.2$–0.4, so that the average coefficient of ejection of particles from the surface is $K^{\pm} \sim 10$–100.

Another observational test, which permits a direct conclusion about processes which occur near the magnetic poles of the neutron star, is the observation of "relict" γ radiation, i.e., curvature-radiation photons produced in the course of the plasma production. Figure 18 shows the result of a calculation carried out for the pulsar PSR 0833-45 through a solu-

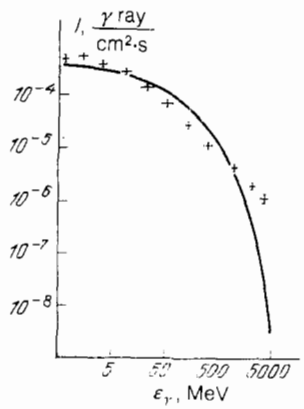

FIG. 18. Spectrum of the "relict" γ radiation, which arises in the course of the production of the e^+e^- plasma. The points are results of observations of the γ emission from the pulsar PSR 0833-45 (Ref. 36).

tion of equations (4.1)–(4.3) for a rotating dipole magnetic field. There is a fair agreement between the calculated results and the observational results obtained on the COS B and SAS-2 satellites for energies[36] $\varepsilon_\gamma \lesssim 1$ GeV. At high energies the spectrum of the relict γ radiation falls off because of the strong single-photon absorption of γ quanta in a magnetic field.[71]

6.3. Evolution; weakly emitting pulsars. The evolution of single pulsars is determined completely by Eqs. (3.35) and (3.36), which determine the rate of change of the period P and the axis inclination angle χ. Using asymptotic expression (6.11), we find, for pulsars with $Q < 1$,

$$\dot{P}_{-15} \approx B_{12}^{10/7} P^{1/14} \cos^{2d} \chi, \tag{6.17}$$

$$\dot{\chi} \approx B_{12}^{10/7} \cos^{2d-1}\chi P^{1/14} \frac{\sin \chi_0}{P_0}, \tag{6.18}$$

where χ_0 and P_0 are the initial values of the inclination angle χ and of the period P, and $d \approx 0.7$–0.8 is a slowly varying function of the angle χ (Ref. 41). As we have already mentioned, the angle χ increases with time.

Equations (6.17) and (6.18) can be used (first) to determine the so-called braking parameter $n_b \equiv \Omega\ddot{\Omega}/\dot{\Omega}^2$:

$$n_b = 2 + 2d \operatorname{tg}^2 \chi, \quad \chi \neq \frac{\pi}{2}, \quad B_{12} < 4.4. \tag{6.19}$$

Knowing n_b, we can also determine the axis inclination angle χ. For the pulsar PSR 1509-58, for example (this is one of the two pulsars for which the braking parameter has been reliably determined[72]), we have $n_b = 2.83 \pm 0.03$ and thus[73]

$$\chi_{1509} = (52 \pm 2)^\circ. \tag{6.20}$$

The value of (6.20) is precisely the same as the value found for the angle χ from an analysis of the x-ray emission profile of this pulsar.[74]

Furthermore, analysis of Eqs. (6.17) and (6.18) shows that pulsars for which the parameter Q was less than unity at the time of their formation go into the region $Q > 1$ [or, equivalently, $\beta_0 \approx \beta_M(\chi)$] after a time $t \approx t_a$, where

$$t_a = 3 \frac{P_0}{\sin \chi_0} B_{12}^{-10/7} \text{ million years}. \tag{6.21}$$

As we have seen, in this region the cascade production of particles is suppressed to a large extent, so that pulsars with $Q > 1$ are in a stage of fading. The time t_a in (6.21) is therefore a characteristic lifetime of a pulsar. For magnetic fields $B_0 \sim 10^{12}$ G, this time would be a few million years. The rotation period at which the pulsar reaches the value $Q = 1$, on the other hand, is

$$P_{cr} \approx B_{12}^{8/15} \text{ s}. \tag{6.22}$$

If a pulsar is formed with a sufficiently short period P_0, it will go into the angular region $\chi \approx 90^\circ$ before it reaches the extinction boundary $\beta_0 \approx \beta_M(\chi)$. If the period of the pulsar is not too long,

$$P \lesssim 0.3 B_{12}^{4/9} \text{ s}, \tag{6.23}$$

its parameter Q will remain less than unity, so that the production of secondary particles will continue to occur.

The primary distinctive feature of such pulsars is that their slowing is determined by an asymmetric current, i.e., by a current which flows away from the star in one part of the polar cap and returns to the star in another part.[40,41] Such a current configuration would be possible only if the angle χ satisfied the condition

$$\left|\chi - \frac{\pi}{2}\right| < \frac{R_0}{R} \approx \left(\frac{\Omega R}{c}\right)^{1/2}. \tag{6.24}$$

The retarding moment due to the asymmetric current is smaller by a factor of at least $(\Omega R/c)$ than the retarding moment described by (3.34) with $\chi \approx 0^\circ$. For this reason, the intensity of the radio emission of such pulsars should also be modest.

In summary, pulsars with angles $\chi \approx 90^\circ$ should have the following features[41]:

a) a fast ($P < 0.1$–0.4 s) or ultrafast ($P < 0.01$ s) rotation;

b) a slight slowing ($\dot{P} \sim 10^{-17} - 10^{-20}$);

c) a weak radio emission ($E_{rad} \sim 10^{24}$–10^{25} erg/s for fast pulsars or $E_{rad} \sim 10^{27}$–10^{28} erg/s for ultrafast pulsars);

d) an "interpulse" ($\chi \approx 90^\circ$);

e) a reduced magnetic field B_0.

We see that at the present sensitivity level of receivers[75] it would be possible to detect only ultrafast, "weakly emitting" pulsars. We do not rule out the possibility that this group would include the recently discovered millisecond pulsars[76–78] with periods of 1.56, 5.4, and 6.1 ms, which have extremely small slowing rates, $\dot{P} \sim 10^{-18}$–10^{-19}. An interpulse has been observed for two of these pulsars. It must be recalled, of course, that according to the present theory of the evolution of fast-period pulsars[79] all these pulsars should go through a stage of a binary system, in which the dynamics of their slowing may, generally speaking, differ from that of the slowing of an isolated neutron star. Indeed, two of the three millisecond pulsars are members of binary systems.

With regard to the weakly emitting pulsars with a period $P \sim 0.1$–0.4 s, we note that they could be observed only if the sensitivity of receivers were increased by one or two orders of magnitude beyond that of existing apparatus.

6.4. Statistics of pulsars. For a statistical analysis of pulsars it is convenient to examine their distribution with respect to the magnetic field B, the period P, the axis inclination angle χ, and the time t: $N(P,\chi,B,t)$. The change in the distribution function is described in this case by the kinetic equation

$$\frac{\partial N}{\partial t} + \frac{\partial}{\partial P}\left(N \frac{dP}{dt}\right) + \frac{\partial}{\partial \chi}\left(N \frac{d\chi}{dt}\right) = U - V; \tag{6.25}$$

here dP/dt and $d\chi/dt$ are determined in accordance with (3.35) and (3.36), i.e., are known functions of B, P, and χ. The source U on the right side of (6.25) describes the formation of pulsars, while V describes their disappearance (extinguishing).

The time scale of the changes in the source U, which is determined by the average lifetime of the stars, is much longer than the pulsar lifetime in (6.21). The distribution function of the pulsars can therefore be assumed quasisteady—independent of the time. For simplicity we will assume here

that the source U depends on P and B independently and is equiprobable in the initial angle χ:

$$U = \frac{2}{\pi} U_{\rm P}(P)\, U_{\rm B}(B). \tag{6.26}$$

The sink function V should be zero everywhere except in the pulsar fading region, i.e., in the region of parameter values corresponding to the condition $Q > 1$. It is thus convenient to consider only pulsars with $Q < 1$, for which we can set $V = 0$. In this case the "sink" is the region of parameter values corresponding to the condition $\beta_0 = \beta_{\rm M}(\chi)$.

Now substituting asymptotic expressions (6.17) and (6.18)—which hold specifically for pulsars with $Q < 1$—into kinetic equation (6.25), and using the integral of motion in (3.36), we finally find the steady-state distribution function

$$N(P,\ \chi,\ B) = \frac{2}{\pi} \frac{U_{\rm B}(B)}{B_{12}^{10/7} P \cos^{2d-1}\chi} \times \int_0^P \frac{P' U_{\rm P}(P')\, {\rm d}P'}{[1-(\sin^2\chi P'^2/P^2)]^{1/2}} \Theta_1(\beta_{\rm M} - \beta_0). \tag{6.27}$$

The step function $\Theta_1[\beta_{\rm M} - \beta_0(P,\chi,B)]$ selects pulsars with $Q < 1$.

We wish to stress that distribution function (6.27) is not the expected distribution function of the observable pulsars. Radio emission can be detected only if the flux density in the pulse, I_ν, exceeds a certain value $I_\nu^{(0)}(P, {\rm DM}, \ldots)$, which characterizes the given radiation receiver (DM is a dispersion measure of the pulsar). In particular, it would be impossible to observe a pulsar if the earth did not lie in its directional pattern. The distribution function of the observable pulsars, $N_0(P,\chi,B)$ is therefore related to the steady-state function in (6.27) by a relation of the form

$$N_0 = NA, \tag{6.28}$$

where $A(I_\nu^{(0)}, DM, \ldots)$ is an observability coefficient. For simplicity we will use the simple function[25]

$$A = \pi \sin\chi \frac{W_r^0(P)}{360^\circ} \tag{6.29}$$

[W_r^0 (degrees) is the width of the window of observable radiation], which reflects only the geometric properties of the directional pattern. More-accurate expressions for A, incorporating the particular features of various receivers, are given by Lyne *et al.*[14]

A systematic comparison of the observational data with the theory thus requires knowledge of both the pulsar distribution function $N(P,\chi,B)$ and the observability coefficient A. Knowing the functions $N(P,\chi,B)$ and A, on the other hand, we can determine the statistical characteristics of pulsars as averages over the distribution function $N_0(P,\chi,B)$. In particular, this approach makes it possible to reconstruct the source functions $U_{\rm P}(P)$ and $U_{\rm B}(B)$.

Analysis of Eqs. (6.27) and (6.29) shows that the observed pulsar distribution agrees quite well with the assumption that the source function satisfies $U_{\rm P}(P) = U_{\rm P} = {\rm const}$, i.e., that the initial periods of the pulsars are equiprobable (this assumption agrees with the results of Refs. 80 and 81). Only in this case does the distribution function $N_0(P)$ fall off at small values of P, as the observed pulsar distribution (Fig. 16) does. It has now been established[82] that this deficiency of pulsars at $P < 0.3$ s reflects an actual decrease in the number of pulsars with small periods and is not a consequence of observational selection.

The source function $U_{\rm B}(B)$, on the other hand, turns out to be relatively insensitive to changes in the other parameters. The function

$$U_{\rm B}(B) = \frac{\Gamma(\bar\gamma+\bar\beta+1)}{\Gamma(\bar\gamma+1)\Gamma(\bar\beta)} \frac{1}{B_0} \left(\frac{B}{B_0}\right)^{\bar\gamma} \left(1 + \frac{B}{B_0}\right)^{-1-\bar\gamma-\bar\beta} \tag{6.30}$$

provides a rather good interpolation of the source function $U_{\rm B}(B)$; the parameters $\bar\gamma$, $\bar\beta$ and B_0 will be determined below.

Now using relations (6.27)–(6.30) and the fact that the window width W_r^0 for pulsars with $Q < 1$ can be written as $W_r^0 = W_0 P^{\bar\upsilon}$, where (Ref. 70, for example)

$$\bar\upsilon = -0.2 \pm 0.1, \tag{6.31}$$

we finally find the following expression for the distribution function in (6.28):

$$N_0(P,\ \chi,\ B) = k_N N P^{\bar\upsilon+1} \frac{1}{B_0} \left(\frac{B}{B_0}\right)^{\bar\gamma-(10/7)} \times \left(1 + \frac{B}{B_0}\right)^{-1-\bar\gamma-\bar\beta} F_d(\chi)\, \Theta_1(\beta_{\rm M} - \beta_0), \tag{6.32}$$

where $F_d(\chi) = 2(1-\cos\chi)\cos^{1-2d}\chi/\sin\chi$, N is the total number of pulsars, and k_N is a normalization factor of order unity.

We will now use three examples to show how distribution function (6.32) can be used to compare the theoretical predictions with observational data. We first need to say a few words about the evolution of the magnetic field. The model developed above is based on the assumption that the magnetic field of each pulsar remains constant over the lifetime of the pulsar. To verify this assumption, we separately analyzed the distributions in the magnetic field for "old" ($Q > 1$) and "young" ($Q < 1$) pulsars. For pulsars with $Q < 1$ we find, integrating distribution function (6.32) over P and χ,

$$N_0(B) \propto \left(\frac{B}{B_0}\right)^{(8/15)(\bar\upsilon+2)-(10/7)+\bar\gamma} \left(1 + \frac{B}{B_0}\right)^{-1-\bar\gamma-\bar\beta}, \quad Q < 1. \tag{6.33}$$

For pulsars with $Q > 1$, on the other hand, projecting distribution function (6.32) onto the boundary $\beta_0 = \beta_{\rm M}(\chi)$ (according to our assumption, all pulsars with $Q > 1$ are at this boundary), we find

$$N_0(B) \propto \left(\frac{B}{B_0}\right)^{(8/15)(\bar\upsilon+1)-(10/7)+\bar\gamma} \left(1 + \frac{B}{B_0}\right)^{-1-\bar\gamma-\bar\beta}, \quad Q > 1. \tag{6.34}$$

Figure 19 compares distribution functions (6.33) and (6.34) with the observed distribution of pulsars in the magnetic field B, determined from (6.14) and (6.15). We see that for both old and young pulsars there is good agreement between theory and observation, confirming our assumption

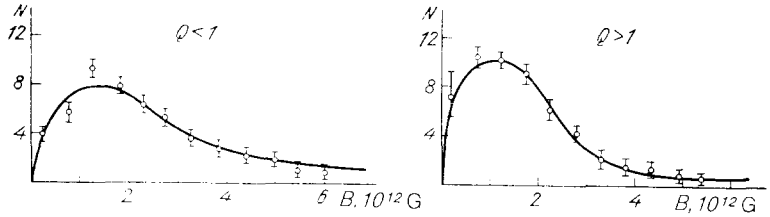

FIG. 19. Distribution of pulsars with respect to the magnetic field B_0. Solid lines—theoretical distributions (6.33) and (6.34); points—observations.

that the magnetic field remains constant. The best parameter values in the function $U_B(B)$ are

$$\bar{\gamma} = 2, \quad \bar{\beta} = 0.75, \; B_0 = 10^{12}\ \text{G}. \tag{6.35}$$

The apparent reason for the constancy of the magnetic field is the relatively short duration of the active life of a pulsar, given by (6.21), over which the magnetic field does not have time to change substantially. We wish to stress that an analysis of the evolution of pulsars on the basis of the equations for magnetic dipole radiation (3.38), led to the opposite conclusion.[83,84] In addition, we can determine the number of "interpulse" pulsars, i.e., pulsars for which the condition $|(\pi/2) - \chi| < W_r$ holds, so that radio emission can be detected from both magnetic poles. The observed dependence of the relative number of interpulse pulsars, N_{inter}/N, on the period P is shown in Fig. 20 along with the expected distribution found with the help of distribution function (6.32). The theory thus not only correctly determines the total number of pulsars with interpulses but also successfully explains the dependence of their relative number, N_{inter}/N, on the period.[41]

We recall that the absence of pulsars with an interpulse at large periods, $P > 1$ s, is a consequence of the fact that such pulsars reach the extinction boundary $\beta_0 = \beta_M(\chi)$ at angles χ considerably smaller than 90°. In contrast, at small values of P, most of the observable pulsars should have an interpulse. As can be seen from (6.21), neutron stars with rotation periods $P < 1$ s move quite quickly into the angular region $\chi \approx 90°$, where they effectively accumulate.

Finally, Fig. 21 shows the observed distribution of pulsars with $Q < 1$ with respect to the value of $W = I_r \Omega\dot{\Omega}$, which is the total power lost by the neutron star. We see that over the broad loss range $W \sim 10^{31}$–10^{34} erg/s this distribution is described by a power law[85] $N(W) \alpha W^{-\bar{\nu}}$, where

$$\bar{\nu}_{\text{obs}} = 1.58 \pm 0.03. \tag{6.36}$$

Distribution function (6.32), which follows from the theory, also leads to a power-law functional dependence $N_0(W)$. The exponent $\bar{\nu}_{\text{theor}} \equiv 1.68 = 0.34\bar{v}$ is determined exclusively by the rather well-known quantity $\bar{v}$, given in (6.31), and is independent of the nature of the source function $U_B(B)$, in (6.30) and (6.35). For the values of $\bar{v}$ which follow from (6.31) we find

$$\bar{\nu}_{\text{theor}} = 1.60 \pm 0.03, \tag{6.37}$$

which, we see, is again in agreement with observational data.

6.5. Radio emission. We conclude by comparing the basic properties of the observed radio emission with the theoretical conclusions.

As was shown in §5, the characteristic frequencies for which the amplification of unstable curvature-plasma waves is most effective are the same as the frequencies of the observed radio emission (Fig. 14). Furthermore, since the amplification of such modes is limited by nonlinear processes, as has been shown, the intensity of the radio emission should be a certain fraction of the total energy of the plasma which flows in the inner regions of the magnetosphere of the pulsar. Accordingly, the conversion coefficient α, which is the ratio of the radio luminosity E_{rad} to the energy W_p which is expended on plasma production, given in (3.37), must on the average remain constant for all pulsars.

Figure 22 shows the distributions of pulsars with $Q < 1$ (solid line) and with $Q > 1$ (dashed line) as functions of the

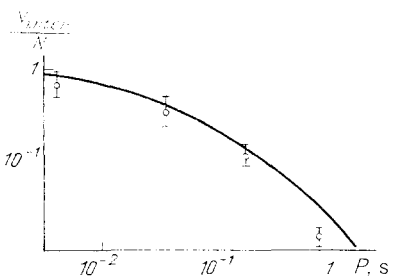

FIG. 20. Relative number of pulsars having an interpulse as a function of the period P.

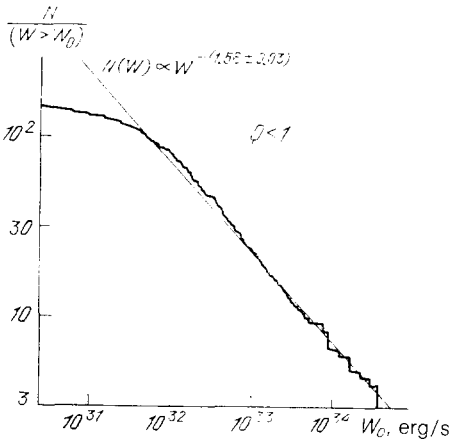

FIG. 21. Integrated distribution of pulsars with $Q < 1$ with respect to the quantity $W = I_r \Omega\dot{\Omega}$, i.e., the total power lost by the neutron star.

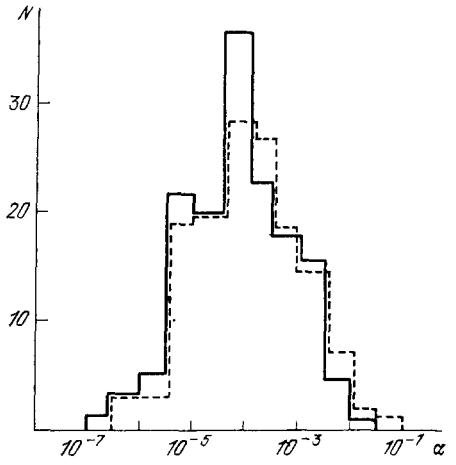

FIG. 22. Distributions with respect to the conversion coefficient α for pulsars with $Q<1$ (solid line) and for those with $Q>1$ (dashed line).

conversion coefficient α. The value of α was found directly from observations, since we have, according to (3.37),

$$\alpha \equiv \frac{E_{\text{rad}}}{W_{\text{p}}} = \frac{E_{\text{rad}}}{W}\frac{W}{W_{\text{p}}} = \frac{E_{\text{rad}}}{I_{\text{r}}\Omega\dot{\Omega}}\frac{\beta_{\text{M}}(\chi)}{\beta_0}; \qquad (6.38)$$

here $W = I_{\text{r}}\Omega\dot{\Omega}$ is the total power loss of the neutron star, given by (3.37), and the ratio $\beta_0/\beta_{\text{M}}(\chi)$ is related to Q by virtue of (6.12). [For $Q>1$, we have $\beta_0 \approx \beta_{\text{M}}(\chi)$, as we have already mentioned.]

These distributions are seen to be essentially the same. Consequently, the conversion coefficient α is indeed a universal characteristic, which does not depend (in particular) on the period P. This constancy of α indicates the existence of a common mechanism for the radio emission of all pulsars. The average value of the conversion coefficient α is

$$\alpha \sim 10^{-4}. \qquad (6.39)$$

With regard to the ratio $E_{\text{rad}}/I_{\text{r}}\Omega\dot{\Omega}$, we note that for fast-period pulsars it should be one or two orders of magnitude smaller than that for pulsars with $P\sim 1$ s, as can be seen from (6.38) (Refs. 70 and 86). The reason is that for pulsars with $P<1$ s, for most of which the relations $Q\ll 1$ and $\beta_0 \ll \beta_{\text{M}}(\chi)$ hold, the particles inside the light cylinder carry only a small fraction of the total loss of rotational energy of the star.

The theory also yields the basic geometric properties of the observed radio emission. For example, if we assume that the conversion of unstable curvature-plasma modes into transverse electromagnetic waves occurs at a height of the order of r_{M}, determined by (5.21), we find the following expression for the width of the directional pattern of the radio emission:

$$W_{\text{r}}^0 = 22°\lambda_3^{1/6}\gamma_{300}^{-1/2}P^{-1/2}\nu_{\text{GHz}}^{-1/6}\left(\frac{f}{f^*}\right)^{1/3}. \qquad (6.40)$$

As we will see, the quantity W_{r}^0 is the same as the characteristic width of the mean profiles of pulsars (Fig. 2).

Furthermore, relation (6.40) yields an explanation of the observed dependence of the width of the mean profiles, W_{r}^0, on the frequency ν and the period P of the pulsar: According to (6.40), the value of W for each pulsar should depend on the frequency ν in a power-law fashion, with $W_{\text{r}}^0 \propto \nu^{-1/6}$. This behavior is in fact observed, both on the average over the range from 400 MHz to 4 GHz [in which we have $W_{\text{r}}^0 \propto \nu^{-(0.15\pm 0.05)}$, according to Ref. 87] and for many individual pulsars over a significantly broader frequency range.[88] The dependence of the window width W_{r}^0 on the period P is determined not only by the power-law factor $P^{-1/2}$ but also by the way in which the value of the line of force f_{patt}, which determines the angular size of the directional pattern of the radio emission, depends on the period. For pulsars with $Q>1$, for example, for which we have $f_{\text{patt}} \approx f^*$, we find $W_{\text{r}}^0 \propto P^{-1/2}$. From the results of Ref. 70 we have $W_{\text{r}}^0 \propto \nu^{-(0.46\pm 0.05)}$, in complete agreement with the theoretical prediction. For pulsars with $Q<1$, on the other hand, the width of the directional pattern should be determined by the inner radius of the hollow cone, given in (6.5), where there is an intense jet of a surface current I_{in}, given in (6.8) (Ref. 41). Consequently, the P dependence of W_{r}^0 becomes slightly different [see (6.31)].

Furthermore, if the maximum of the radio emission does in fact lie near $r_\perp = r_{\text{in}}$, then all the pulsars for which the line of sight intersects the directional pattern far from the inner radius of the hollow cone should have a simple single profile. For only those pulsars for which the relation $r_{\perp\min} < r_{\text{in}}$ holds should the observed profile be binary. Some examples of mean profiles of this sort are shown in Fig. 2.

Clearly, for a given inner radius of the hollow cone, r_{in}, the ratio of the number of pulsars with simple and binary profiles should be

$$\frac{N_1}{N_2} = \frac{R_0 - r_{\text{in}}}{r_{\text{in}}} = \frac{R_0}{r_{\text{in}}} - 1, \qquad (6.41)$$

and according to (6.13) it can be expressed directly in terms of the observable quantity Q. From Fig. 23 we see that here again there is good agreement between theory and observations.[41]

Finally, the theory also explains the basic polarization properties of the radio emission. As was shown in §4, in the inner part of the magnetosphere (region III in Fig. 12) only two transverse, linearly polarized waves can propagate; only one of them can effectively interact with unstable curvature-plasma modes. Therefore, the radio emission from pulsars

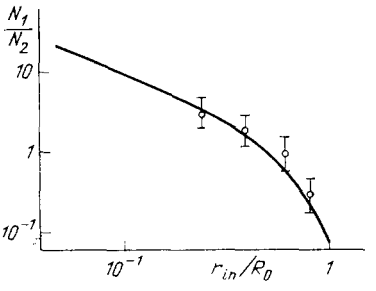

FIG. 23. Relative number of pulsars with single and binary mean profiles, N_1/N_2, as a function of the parameter r_{in}/R_0. The curve shows the expected dependence, given by (6.41).

should have a significant linear polarization, with a position angle determined by the projection of the magnetic field onto the visual plane. As we know, this model also gives a good explanation of the observed behavior of the position angle, shown in Fig. 3 (Refs. 25 and 89).

7. CONCLUSION

In summary, the theory given above makes substantial progress toward an understanding of the basic physical processes which occur in the magnetosphere of a neutron star. This theory has been used to determine the basic properties of the dynamics and evolution of pulsars and to determine the nature of their activity, in particular, to find a coherent mechanism for the observed emission. The basic theoretical predictions agree with observational data, as has been shown.

There are of course many other questions which require detailed theoretical study, e.g., the effect of nonlinear processes on the characteristics of the radio emission, the origin of the subpulse and microstructural details, the correlation properties of the former, and the origin of the ultrahigh-energy γ rays. On the whole, however, the physical picture of the basic processes which occur in the magnetosphere of a pulsar seems to be clear.

[1)] *Transl. ed. note*: The term "curvature radiation" (similar to, but distinct from "synchrotron radiation") is used by Sturrock[41] and in later references, and is described in Sec. 4 of this paper.

[2)] More precisely, L varies with the axis inclination angle χ, from 0.33 at $\chi = 0°$ to 0.48 at $\chi = 90°$.

[3)] In ultrastrong magnetic fields $B \gtrsim B_c$ (i.e., $B_\hbar \gtrsim 1$), which have been studied by Shabad and Usov,[62,63] the dispersion of the photons is markedly different than that in vacuum, and positronium can form. These processes will not be discussed in the present paper.

[4)] According to Ref. 42, there is also a weak dependence of Ψ_c and H on the logarithmic parameter Λ at $B_\hbar < (2/3)\Lambda^{-1}$. Here we are setting $\Lambda = 8$. At $B_\hbar > (2/3)\Lambda^{-1}$, we would replace (4.18) by another expression.[42]

[1]A. Hewish, S. J. Bell, J. D. H. Pilkington, P. F. Scott, and R. A. Collins, Nature, **217**, 709 (1968) [Russ. transl., Usp. Fiz. Nauk **95**, 705 (1968)].
[2]T. Gold, Nature **218**, 731 (1968).
[3]V. R. Pandharipande, D. Pines, and R. A. Smith, Astrophys. J. **208**, 550 (1976).
[4]W. Baade and F. Zwicky, Proc. Nat. Acad. Sci. **20**, 254 (1934).
[5]R. Giacconi, Ann. N. Y. Acad. Sci. **262**, 312 (1975).
[6]O. P. Babushkina, L. S. Bratolyubova-Tsulukidze, R. N. Izrailovich, M. I. Kudryavtsev, A. S. Meshoronskiĭ, I. A. Savenko, and V. M. Shamonin, Pis'ma Astron. Zh. **1**, No. 6 (1975).
[7]R. W. Klebesadel, I. B. Strong, and R. A. Olson, Astrophys. J. **182**, L85 (1973).
[8]B. Margon, H. C. Ford, J. I. Katz, K. B. Kwitter, R. K. Ulrich, R. P. G. Stone, and A. Klemola, Astrophys. J. **230**, L41 (1979).
[9]R. Giacconi, P. Gorenstein, H. Gurski, and J. R. Waters, Astrophys. J **148**, L119 (1967).
[10]C. H. Townes, J. H. Lacy, T. R. Geballe, and D. J. Hollenbach, Nature **301**, 661 (1983).
[11]I. L. Rozental', V. V. Usov, and I. V. Éstulin, Usp. Fiz. Nauk **140**, 97 (1983) [Sov. Phys. Usp. **26**, 437 (1983)].
[12]P. R. Amnuél', Nebo v Rentgenovskikh Luchakh (The x-Ray Sky), Nauka, Moscow, 1984.
[13]V. M. Vladimirskiĭ, A. M. Gal'per, B. I. Luchkov, and A. A. Stepanyan, Usp. Fiz. Nauk **145**, 255 (1985) [Sov. Phys. Usp. **28**, 153 (1985)].
[14]A. G. Lyne, R. N. Manchester, and J. H. Taylor, Mon. Not. R. Astron. Soc. **213**, 613 (1985).
[15]J. G. Davies, A. G. Lyne, and J. H. Seiradakis, Mon. Not. R. Astron. Soc. **179**, 635 (1977).
[16]B. Anderson and A. G. Lyne, Nature **303**, 597 (1983).
[17]J. M. Weisberg, J. H. Taylor, and L. A. Fowler, Sci. Am. **245(4)**, 74 (October 1982) [Russ. transl., Usp. Fiz. Nauk **137**, 707 (1982)].
[18]A. N. Hall, Mon. Not. R. Astron. Soc. **191**, 739 (1980).
[19]N. A. Lotova and I. V. Chashey, Astrophys. Space Sci. **32**, 331 (1975).
[20]A. A. Ruzmaikin and D. D. Sokolov, Astron. Astrophys. **58**, 247 (1977).
[21]J. H. Taylor and D. R. Stinebring, Ann. Rev. Astron. Astrophys. (1968).
[22]M. M. Davis, J. H. Taylor, J. M. Weisberg, and D. C. Backer, Nature **315**, 547 (1985).
[23]V. G. Il'in, Yu. P. Ilyasov, A. D. Kuz'min, S. B. Pushkin, G. N. Paliĭ, T. V. Shabanova, and Yu. P. Shitov, Dokl. Akad. Nauk SSSR **275**, 835 (1984) [Sov. Phys. Dokl. **29**, 252 (1984)].
[24]O. Kh. Guseĭnov and I. M. Yusifov, Astron. Zh. **61**, 708 (1984) [Sov. Astron. **28**, 415 (1984)].
[25]R. Manchester and J. Taylor, *Pulsars*, Freeman, San Francisco, 1977 (Russ. transl., Mir, M., 1980).
[26]J. M. Rankin, Astrophys. J. **274**, 333 (1983).
[27]B. J. Rickett, T. H. Hankins, and J. M. Cordes, Astrophys. J. **201**, 425 (1975).
[28]T. V. Smirnova, V. A. Soglasnov, M. V. Popov, and A. Yu. Novikov, Astron. Zh. **63**, 84 (1986) [Sov. Astron. **30**, 51 (1986)].
[29]R. N. Manchester, J. H. Taylor, and G. R. Huguenin, Astrophys. J. **196**, 83 (1975).
[30]P. A. Hamilton, P. M. McCalloch, J. G. Ables, and M. M. Komesaroff, Mon. Not. R. Astron. Soc. **180**, 1 (1977).
[31]D. R. Stinebring, J. M. Cordes, J. M. Rankin, J. M. Weisberg, and V. Boriakoff, Astrophys. J. Suppl. **55**, 521 (1984).
[32]W. Sieber, Astron. Astrophys. **28**, 237 (1973).
[33]V. A. Izvekova, A. D. Kuzmin, V. M. Malofeev, and Yu. P. Shitov, Astrophys. and Space Sci. **78**, 45 (1981).
[34]V. L. Ginzburg, V. V. Zheleznyakov, and V. V. Zaĭtsev, Usp. Fiz. Nauk **98**, 201 (1969) [Sov. Phys. Usp. **12**, 378 (1969)].
[35]V. L. Ginzburg, Usp. Fiz. Nauk **103**, 393 (1971) [Sov. Phys. Usp. **14**, 83 (1971)].
[36]G. Kanbach, K. Bennet, G. F. Bignami *et al.*, Astron. and Astrophys. **90**, 163 (1980).
[37]F. K. Knight, Astrophys. J. **260**, 538 (1982).
[38]P. Goldreich and W. H. Julian, Astrophys. J. **157**, 869 (1969).
[39]F. C. Michel, Rev. Mod. Phys. **54**, 1 (1982).
[40]V. S. Beskin, A. V. Gurevich, and Ya. N. Istomin, Zh. Eksp. Teor. Fiz. **85**, 401 (1983) [Sov. Phys. JETP **58**, 235 (1983)].
[41]V. S. Beskin, A. V. Gurevich, and Ya. N. Istomin, Astrophys. and Space Sci. **102**, 301 (1984).
[42]A. V. Gurevich and Ya. N. Istomin, Zh. Eksp. Teor. Fiz. **89**, 3 (1985) [Sov. Phys. JETP **62**, 1 (1985)].
[43]P. A. Sturrock, Astrophys. J. **164**, 529 (1971).
[44]J. K. Daugherty and A. K. Harding, Astrophys. J. **252**, 337 (1982).
[45]V. S. Beskin, A. V. Gurevich, and Ya. N. Istomin, Pis'ma Zh. Eksp. Teor. Fiz. **44**, 18 (1986) [JETP Lett. **44**, 20 (1986)].
[46]D. Pines, J. Phys. (Paris) C. 2, 111 (1980) [Russ. transl., Usp. Fiz. Nauk **131**, 479 (1980)].
[47]R. D. Blandford, J. H. Applegate, and L. Hernguist, Mon. Not. R. Astron. Soc. **204**, 1025 (1983).
[48]M. S. Strickman, J. D. Kurfess, and W. N. Johnson, Astrophys. J. **254**, L23 (1982).
[49]F. C. Michel, Astrophys. J. **180**, 207 (1973).
[50]L. Mestel and Y. M. Wang, Mon. Not. R. Astron. Soc. **188**, 799 (1979).
[51]A. V. Gurevich, A. L. Krylov, and E. E. Tsedilina, Space Sci. Rev. **19**, 59 (1976).
[52]H. Heintzmann, Nature **292**, 811 (1981).
[53]J. P. Ostriker and J. E. Gunn, Astrophys. J. **157**, 1395 (1969).
[54]M. A. Ruderman and P. G. Sutherland, Astrophys. J. **196**, 51 (1975).
[55]E. Tademaru, Astrophys. J. **183**, 625 (1973).
[56]E. T. Scharlemann, J. Arons, and W. M. Fawley, Astrophys. J. **222**, 297 (1978).
[57]J. Arons and E. T. Scharlemann, Astrophys. J. **231**, 854 (1979).
[58]J. Arons, Astrophys. J. **266**, 215 (1983).
[59]P. B. Jones, Mon. Not. R. Astron. Soc. **197**, 1103 (1981).
[60]L. D. Landau and E. M. Lifshitz, Kvantovaya Élektrodinamika, Nauka, Moscow, 1980 (V. B. Berestetskiĭ, E. M. Lifshitz, and L. P. Pitaevskiĭ, Quantum Electrodynamics, Pergamon, New York, 1982).
[61]Yu. P. Ochelkov and V. V. Usov, Astrophys. and Space Sci. **69**, 439 (1980).
[62]A. E. Shabad and V. V. Usov, Astrophys. and Space Sci. **102**, 327 (1984).

[63]V. V. Usov and A. E. Shabad, Pis'ma Zh. Eksp. Teor. Fiz. **42**, 17 (1985) [JETP Lett. **42**, 19 (1985)].
[64]R. D. Blandford, Mon. Not. R. Astron. Soc. **170**, 551 (1975).
[65]D. G. Lominadze, A. B. Mikhaĭlovskiĭ, and R. Z. Sagdeev, Zh. Eksp. Teor. Fiz. **77**, 1951 (1979) [Sov. Phys. JETP **50**, 927 (1979)].
[66]V. E. Shaposhnikov, Astrofizika **17**, 749 (1981).
[67]J. G. Lominadze, G. Z. Machabeli, and V. V. Usov, Astrophys. and Space Sci. **90**, 19 (1983).
[68]E. Asseo, R. Pellat, and H. Sol, Astrophys. J. **266**, 201 (1983).
[69]V. D. Shafranov, in: Voprosy teorii plazmy, Vol. 3, Gosatomizdat, M., 1963, p. 3 (Reviews of Plasma Physics, Vol. 3, Consultants Bureau, New York, 1967, p. 1).
[70]I. F. Malov and S. A. Suleĭmanova, Astrofizika **18**, 107 (1982).
[71]A. K. Harding, E. Tademaru, and L. W. Esposito, Astrophys. J. **225**, 226 (1978).
[72]R. Manchester, J. M. Durdin, and L. M. Newton, Nature **313**, 376 (1985).
[73]Ya. N. Istomin, Pis'ma Astron. Zh. (1986) [*sic*].
[74]F. D. Seward and F. R. Harnden, Astrophys. J. **256**, L45 (1982).
[75]G. H. Stokes, J. H. Taylor, J. M. Weisberg, and R. J. Dewey, Nature **317**, 787 (1985).
[76]D. C. Backer, S. R. Kulkarni, C. Heiles, M. M. Davis, and W. M. Goss, Nature **300**, 615 (1982).
[77]V. Boriakoff, R. Buccheri, and F. Fauci, Nature **304**, 417 (1983).
[78]D. J. Segelstein, L. A. Rawley, D. R. Stinebring, A. S. Fruchter, and J. H. Taylor, Nature (1986).
[79]E. P. J. Van den Heuvel, Astrophys. and Astron. **5**, 209 (1984).
[80]M. Vivekanand and R. Narayan, Astrophys. and Astron. **2**, 315 (1981).
[81]M. A. Mnatsakanyan, Astrofizika **15**, 515 (1979).
[82]R. J. Dewey, J. H. Taylor, J. M. Weisberg, and G. H. Stokes, Astrophys. J. **294**, L25 (1985).
[83]E. Flowers and M. A. Ruderman, Astrophys. J. **215**, 302 (1977).
[84]F. S. Fujimura and C. F. Kennel, Astrophys. J. **236**, 242 (1980).
[85]Yu. I. Neshpor, Astron. Zh. **62**, 408 (1985) [Sov. Astron. **29**, 237 (1985).
[86]I. F. Malov and V. M. Malofeev, Astrophys. and Space Sci. **78**, 73 (1981).
[87]A. D. Kuzmin, V. M. Malofeev, V. A. Izvekova, W. Sieber, and R. Wielebinski, Astron. and Astrophys. (1986).
[88]J. M. Rankin, Astrophys. J. **274**, 359 (1983).
[89]V. Radhakrishnan and D. J. Cocke, Astrophys. Lett. **3**, 225 (1969).

Translated by Dave Parsons